

Review

# Design of DNA-Based Artificial Transmembrane Channels for Biosensing and Biomedical Applications

Wanyu Xu, Hui Chen, Yang Li, Shuangna Liu, Kemin Wang \* and Jianbo Liu \* 

State Key Laboratory of Chemo/Biosensing and Chemometrics, Key Laboratory for Bio-Nanotechnology and Molecular Engineering of Hunan Province, College of Chemistry and Chemical Engineering, Hunan University, Changsha 410082, China; 1349376793@hnu.edu.cn (W.X.); chenhui\_0908@163.com (H.C.);

ly2353345079@163.com (Y.L.); liushuangna@hnu.edu.cn (S.L.)

\* Correspondence: kmwang@hnu.edu.cn (K.W.); liujianbo@hnu.edu.cn (J.L.)

**Abstract:** Biomolecular channels on the cell membrane are essential for transporting substances across the membrane to maintain cell physiological activity. Artificial transmembrane channels used to mimic biological membrane channels can regulate intra/extracellular ionic and molecular homeostasis, and they elucidate cellular structures and functionalities. Due to their program design, facile preparation, and high biocompatibility, DNA nanostructures have been widely used as scaffolds for the design of artificial transmembrane channels and exploited for ionic and molecular transport and biomedical applications. DNA-based artificial channels can be designed from two structural modules: DNA nanotubes/nanopores as transport modules for mass transportation and hydrophobic segments as anchor modules for membrane immobilization. In this review, various lipophilic modification strategies for the design of DNA channels and membrane insertion are outlined. Several types of DNA transmembrane channels are systematically summarized, including DNA wireframe channels, DNA helix bundle channels, DNA tile channels, DNA origami channels, and so on. We then discuss efforts to exploit them in biosensor and biomedical applications. For example, ligand-gated and environmental stimuli-responsive artificial transmembrane channels have been designed for transmembrane signal transduction. DNA-based artificial channels have been developed for cell mimicry and the regulation of cell behaviors. Finally, we provide some perspectives on the challenges and future developments of artificial transmembrane channel research in biomimetic science and biomedical applications.

**Keywords:** artificial transmembrane channel; DNA nanostructure; biosensing; biomedical application



**Citation:** Xu, W.; Chen, H.; Li, Y.; Liu, S.; Wang, K.; Liu, J. Design of DNA-Based Artificial Transmembrane Channels for Biosensing and Biomedical Applications. *Chemosensors* **2023**, *11*, 508. <https://doi.org/10.3390/chemosensors11090508>

Academic Editor: Barbara Palys

Received: 24 July 2023

Revised: 7 September 2023

Accepted: 15 September 2023

Published: 18 September 2023



**Copyright:** © 2023 by the authors. Licensee MDPI, Basel, Switzerland. This article is an open access article distributed under the terms and conditions of the Creative Commons Attribution (CC BY) license (<https://creativecommons.org/licenses/by/4.0/>).

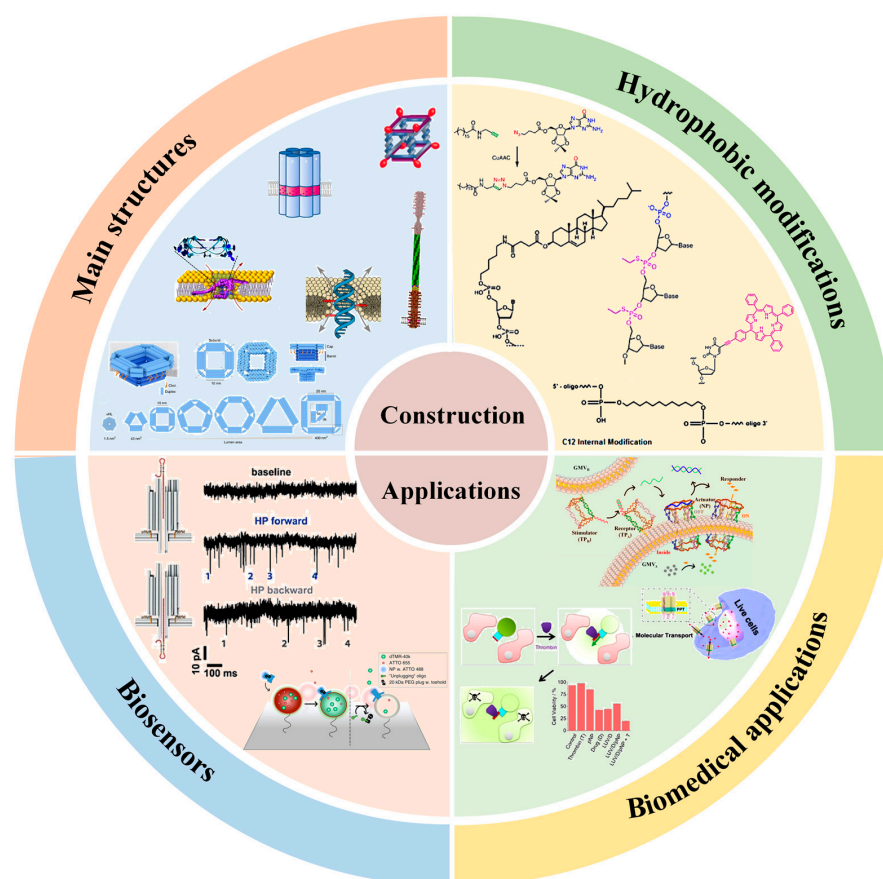
## 1. Introduction

Transmembrane channels are integral membrane proteins with channels or pores that allow particular ions or small molecules to cross a lipid bilayer [1,2]. These channels are critical for regulating ion homeostasis, transporting molecules, maintaining normal cell physiological functions, and performing related life activities [3]. However, their formation requires genetic coding in living cells under strict spatiotemporal control, which is difficult to reproduce in vitro [4]. To date, various materials, such as biological macromolecules, synthetic organic compounds, and inorganic substances, have been successfully used for the design of artificial nanochannels with diverse structures and functions [5]. The design of synthetic biomolecules that mimic the structures and functions of natural transmembrane channels has garnered substantial interest among molecular biology researchers as models for studying fundamental information, creating alternative drugs, and developing advanced biosensors.

Deoxyribonucleic acid (DNA) is an irreplaceable building material for the design of artificial channels [6], since DNA is an easily accessible biomacromolecule with high biocompatibility and programmable self-assembly ability, and it can be safely used in

natural biological processes [7]. In addition, each strand used to construct DNA channels can be independently functionalized through the precise design and modification of various biochemical molecules [8]. With excellent shapes, structures, and functions, DNA-based artificial channels have been widely used for the transmembrane transport of ions or molecules, the transduction of intercellular signals, and the regulation of cell physiological activities [9]. Various methods have been reported for the design of DNA-based transmembrane channels [10]. For example, traditional DNA self-assembly technology has been developed as a simple, practical, and rapid route for designing transmembrane channels, which have been used to simulate signal transduction and ion transport [11–13]. Based on DNA origami technology, the pore size, height, and wall thickness values of the designed DNA channels are relatively easy to customize [14]. Hydrophobic modification of DNA nanostructures is a major design difficulty, but it is necessary to make the DNA channels span the phospholipid bilayer [15]. A regulating switch on the DNA channels can modulate transmembrane transport [16–18].

In this review, we summarize the hydrophobic modification strategies for preparing DNA transmembrane channels in terms of the type, number, and location of hydrophobic modification groups. We systematically summarize the construction of different types of DNA artificial transmembrane channels and discuss their applications in biosensors and biomedicine. (Scheme 1) Finally, we describe the challenges and possible remedies of DNA artificial transmembrane channels in biomimetic science and biomedicine applications and propose some prospects for their future development.



**Scheme 1.** Diagram of the content of the review. DNA-based artificial channels can be designed from two structural modules: DNA nanotubes/nanopores as main structural modules for mass transportation and hydrophobic modifications as anchor modules for membrane immobilization. We systematically summarize the construction of different types of DNA artificial transmembrane channels and discuss their applications in biosensors and biomedicine.

## 2. Hydrophobic Modification for Artificial Transmembrane Channels

The purposes of designing DNA-based artificial channels include the transmembrane transport of substances for signal exchange, the adjustment of the concentrations of substances, and the regulation of cell behaviors. The design method, structure (pore size and length), and interaction force between the channel and phospholipid membrane can directly affect the material transport efficiency [19]. DNA-based artificial transmembrane channels transport ions or biomolecules between phospholipid membranes, which mainly rely on the arrangement and assembly of DNA strands to form nanotubes or nanopores with holes [20]. Generally, DNA-based artificial transmembrane channels are composed of two structural modules: DNA nanotubes/nanopores as transport modules for mass transportation; and hydrophobic segments as anchor modules for membrane immobilization (Figure 1A). For example, phospholipids consist of a hydrophilic head and two hydrophobic tails. Hydrophobic fragments can be inserted into the internal hydrophobic site, allowing DNA nanostructures to be well anchored to phospholipid membranes.

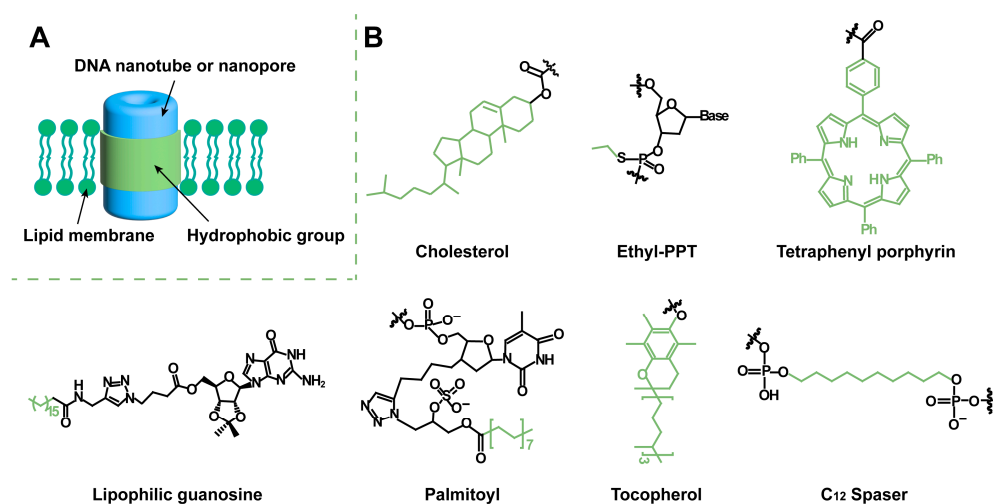


**Figure 1.** Structure model of artificial transmembrane channels and different hydrophobic modifications. (A) Schematic diagram of transmembrane channels formed by hydrophobic-modified DNA nanotubes or nanopores. (B) Various hydrophobic modifications: cholesterol, ethyl-PPT, tetraphenyl porphyrin, lipophilic guanosine, palmitoyl, tocopherol, and C<sub>12</sub> spacer.

A core challenge of DNA nanotubes or nanopores embedded in phospholipid membranes regarding the formation of transmembrane channels is to overcome the adverse interactions between the hydrophilic, negatively charged DNA nanostructures and the hydrophobic membrane environment [6]. Many strategies have been developed to insert DNA nanostructures into the hydrophobic centers of the lipid bilayer. Keyser et al. have proposed several steps for constructing efficient membrane channels, especially for overcoming the high energy barrier of DNA across the bilayer hydrophobic core: (1) The connector between the hydrophobic anchor and the DNA core is shortened to achieve improved control over the anchor position. (2) When large structures are introduced, there should be a large spacing between the hydrophobic anchors to inhibit their simultaneous insertion into the bilayer without inducing crossing [21]. (3) The distance between the end of the structure and the membrane transdomain, as determined by anchor position, is reduced, limiting adverse interactions between the charged material and the hydrophobic core of the membrane [22].

Hydrophobic modification of DNA nanotubes or nanopores is a key step when designing transmembrane channels. Due to the excellent properties resulting from its membrane insertion, cholesterol is the preferred hydrophobic group for DNA modification. Cholesterol is most frequently used because of its strong hydrophobicity and because it can be modified at the DNA end or middle section, which is more conducive to the design of DNA

artificial transmembrane channel structures. The amount and location of cholesterol are adjusted according to the designed channel shape and function. The number of cholesterols on artificial channels has been reported to be in the range of 2–60 [23–30]. DNA channels with small pore sizes and simple structures have little resistance to inserting into the membrane, and the corresponding modification method is relatively simple. Small-aperture artificial channels usually require only a few cholesterols at intervals along the sidewalls of the channel. However, as the pore size increases, it becomes increasingly difficult for DNA channels to be inserted into the lipid membrane. Over 10 cholesterols have been reported to be modified in DNA nanochannels with large apertures [25–30]. Inspired by the first DNA nanochannels, cholesterols are typically modified at the brim of the channel, under the flanking structure, or at the bottom of the middle shell [26–28]. It is necessary to add a coating to sequester cholesterol to prevent channel aggregation and ensure that the DNA channels are individually embedded in the membrane [29].

Ethyl-phosphorothioate (ethyl-PPT) [31], tetraphenyl porphyrin (TPP) [32], lipophilic guanosine [33], palmitoyl [28], tocopherol [34], and C<sub>12</sub> spacer [35] are widely used for DNA hydrophobic modification (Figure 1B). The attachment of the ethyl group to the mercaptan group removes the negative charge of the typical phosphate anion. Ethyl iodide reacts with mercaptan groups through nucleophilic substitution to produce ethyl-protected PPT, which can be used for the hydrophobic modification of DNA channels [31]. To simplify the design of channels and minimize chemical intervention, other chemical labels with improved hydrophobicity have been proposed. It is expected that macroporous channels can be anchored to the membrane with a few chemical labels. TPP meets the requirements of hydrophobicity and can be easily coupled with DNA. Therefore, DNA channels modified with two porphyrin labels are constructed [32]. Acetylene-TPP is rigidly linked to the DNA strand by Sonogashira coupling to deoxyuridine. The T-pore-based artificial channels that were reported in 2016 are hydrophobically modified with tocopherol as a substitute for cholesterol [34]. In addition, biotin-streptavidin-coupled lipid networks have been developed [34]. The biotin-streptavidin connection with the biotinylated lipid membrane provides additional channel-to-membrane interactions, enabling the insertion of single DNA channels into the membrane without channel aggregation.

### 3. Design of DNA Nanostructure for Artificial Transmembrane Channels

Currently, different types of DNA nanostructures have been developed for the design of artificial channels, including DNA wireframes, DNA helix bundles, DNA tiles, DNA origami, and so on.

#### 3.1. DNA Wireframe-Based Transmembrane Channels

DNA wireframe nanotubes are promising self-assembled nanostructures that have produced a range of nanotubes or nanopores with different cavity sizes and tube lengths [36–41]. A typical modular assembly process for designing a wireframe structure from short synthetic strands is as follows: First, DNA structures acting as modular building blocks with specific shapes, such as triangles, squares, pentagons, and hexagons, are designed as needed. DNA nanotube rungs are then formed by longitudinal assembly through connecting strands. By controlling the number of DNA strands in each unit and connecting multiple rungs, the tube can be extended, and DNA nanotubes with micrometer lengths and specific pore shapes can be obtained.

DNA wireframe nanotubes can act as artificial transmembrane channels after adding hydrophobic anchors for membrane insertion. Sleiman et al. [23] designed cuboidal DNA channels and found that changing the pattern of the cholesterol unit on the cuboidal DNA significantly alters its interaction pattern with the lipid membrane (Figure 2A). Modification of cholesterol on a single face of the cube results in the peripheral anchoring of the DNA structure, while modification of cholesterol on two opposite faces of the cube enables the DNA pipeline structure to cross the phospholipid membrane. The DNA channels embedded in the membrane function as nanochannels for the transmembrane transport of

dyes. Furthermore, researchers have designed a switch for the channel to avoid channel aggregation. This switch is achieved by adjusting the length of the cholesterol-DNA conjugate and the interval between the cubic binding segment of the strand and the cholesterol unit. The cholesterol units are initially hidden inside the cube and then exposed by a conformational switch for membrane insertion. Cholesterol-DNA cubes have become the first open-walled DNA channels that can be used as tools for sensing, drug delivery, and cellular behavior regulation applications. The DNA hexagonal prism constructed by Tan et al. [42] can transport ions across the membrane after modifying cholesterol on the four strands of the sidewall. An additional lock strand is designed on the opening side of the channel, and a key strand is added to open the channel for material transport (Figure 2B). These ligand-gated hexagonal DNA nanochannels have been used to mimic bionic ion channels in cell membranes.

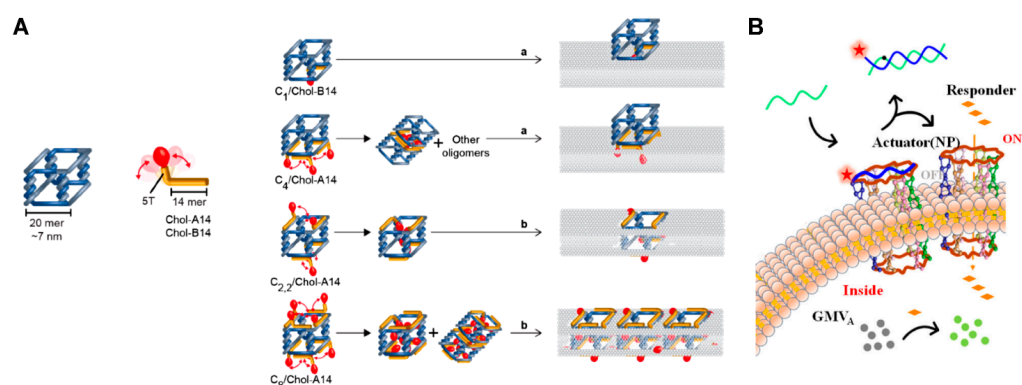


**Figure 2.** DNA wireframe-based transmembrane channels. **(A)** Schematic representation of DNA cube-based transmembrane channels through wireframe assembly. Different amounts of cholesterol-DNA conjugates (yellow lines) bind to the DNA cube at different positions. The cholesterol unit of the cholesterol-DNA conjugate can be flexibly regulated. Every cholesterol-DNA conjugate has 14 bases in the cuboidal binding segment, and an additional 5-thymidine (T) spacer serves as a chain to link the cholesterol, providing flexibility. From top to bottom are cubes containing 1, 4, 2 + 2, and 8 cholesterol-DNA conjugates. The first two images show cubes with cholesterol modified on a single face (a), eventually leading to extramembrane anchoring, and the last two images show cubes with cholesterol modified on two opposing faces (b), which can puncture the membrane. This figure was adapted with permission from ref. [23], copyright 2019, American Chemical Society. **(B)** Schematic diagram of the ligand-gated transmembrane channel response. This figure was adapted with permission from ref. [42], copyright 2021, American Chemical Society.

### 3.2. DNA Helix Bundle-Based Transmembrane Channels

Small-pore DNA-based artificial channels can be designed based on helix bundle (HB)-based nanotube assembly through the concatenation of multiple DNA strands [24]. DNA helix bundles are prepared by cross-joining scaffolds and short strands in the middle or at the ends of the materials, and the helix bundles follow the structural layout of polygon arrays [31]. The six DNA helix bundle (6-HB) nanotubes form approximately 2 nm-wide pores at the center (Figure 3A), which are hydrophobically modified to maintain structural stability in the lipid bilayer and to support a constant transmembrane current (Figure 3B). The reported conductivities of these 6-HB DNA transmembrane channels range from approximately 0.3 nS to 1.6 nS [31,32]. Through molecular dynamics (MD) simulations, the following conclusions are found. (1) The chemical modification on the surface of the channel has an extremely large impact on the transport of water and ions across the membrane, and the type, number, and position of the hydrophobic group modification can directly affect the formation of transmembrane channels. (2) DNA nanochannels can be used to transfer charged solute pairs to antistatic gradients through electroosmosis. (3) The porous channel wall allows the transverse leakage of ions and water. (4) The central lumen of the DNA channel is cylindrical and filled with water and ions; the volumes of water at the opening

regions of both ends fluctuate in time and exhibit mechanosensitive gating (Figure 3C), creating a force sensor [43–46]. The negatively charged channel lumen has a high degree of control over cargo transport. For example, the lumen can act as an  $H^+$  conductor to control the  $H^+$  current [47] and show effective ATTO655 (dye with  $-1$  charge) flux while blocking calcein (dye with  $-4$  charge) transport [37]. Pore transport is affected by surrounding lipids. Studies on charged neutral lipids have shown that 6-carboxyfluorescein (FAM) dye is not transported, but analysis of negatively charged 1-palmitoyl-2-oleoyl phosphatidylglycerol (POPG) shows that FAM dye can be transported by DNA channels [48].

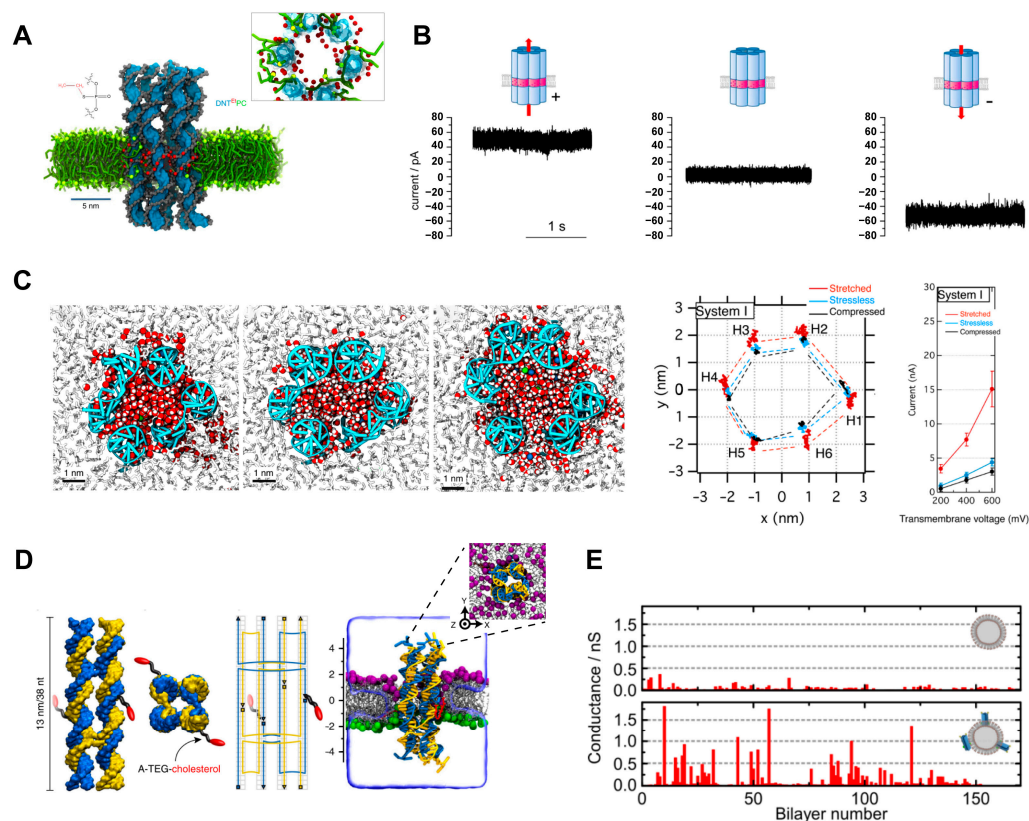


**Figure 3.** DNA helix bundle-based transmembrane channels. (A) Schematic diagram of the molecular simulation of 6-HB-based DNA transmembrane channels modified with ethyl-PPT. Image reproduced with permission from ref. [45], copyright 2017, Springer Nature. (B) Transmembrane current test diagram of the 6-HB DNA nanochannel. From left to right, the current traces of the channel under voltages of +100 mV, 0 mV, and  $-100$  mV are shown. Image reproduced with permission from ref. [31], copyright 2013, American Chemical Society. (C) Simulation diagram, cross-sectional area, and current of the transmembrane channel under compression, zero tension, and compression. Image reproduced with permission from ref. [43], copyright 2015, American Chemical Society. (D) Molecular simulation of the 4-HB transmembrane channel with two cholesterol molecules. Image reproduced with permission from ref. [21], copyright 2018, Springer Nature. (E) Conductivity test diagram of the 4-HB DNA channel. Image reproduced with permission from ref. [49], copyright 2015, American Chemical Society.

In addition, Keyser et al. have constructed a DNA nanochannel with a reduced pore size in which four DNA helical bundles (4-HB) are arranged on a square lattice to form a channel [21,49]. Two of these nonadjacent helical bundles contain a DNA strand carrying terminal cholesterol to embed a channel into the lipid membrane (Figure 3D). In this arrangement, the naturally occurring gaps between the helices produce a central channel with a nominal diameter of approximately 0.8 nm. Conductivity tests confirm the ion conduction ability of 4-HB DNA nanochannels embedded on giant unilamellar vesicles (GUVs). The GUVs embedded with DNA nanochannels are significantly more conductive than pure GUVs (Figure 3E).

### 3.3. DNA Tile-Based Transmembrane Channels

DNA tiles are short intersecting DNA strands that contribute to structural control. They have cohesive ends that can be programmed to self-assemble to form various DNA nanostructures by clinging together [50,51]. DNA tiles have been widely used to prepare DNA nanotubes. The steps of their self-assembly mainly focus on the release of DNA input molecules to trigger the growth of nanostructures, which is a nonautonomous and irreversible reaction [52]. With the maturation of construction technology, several methods have been designed to synthesize DNA tile nanotubes with adjustable, reversible, or controllable termination characteristics [53–55]. By using DNA origami structures as seeds to construct channels, micron-long nanotubes can be obtained through the polymeric growth of DNA tiles. The hydrophobic unit on the seed can directly insert the nanotube into the membrane to form a transmembrane channel (Figure 4A,B) [56]. An additional DNA origami channel cap can be used to terminate the aggregation of tiles. Conductivity measurements reveal that the conductance values of seeds and nanochannels are lower than their uncapped counterparts when the channel caps are attached. The results show that ions move from one end of the channel to the other and that there is partial leakage through the channel wall. However, the observation experiments of fluorescent dyes crossing lipid membranes confirm that molecular transport can occur through DNA nanochannels and that it is mainly end-to-end rather than across the channel wall (Figure 4C) [57].

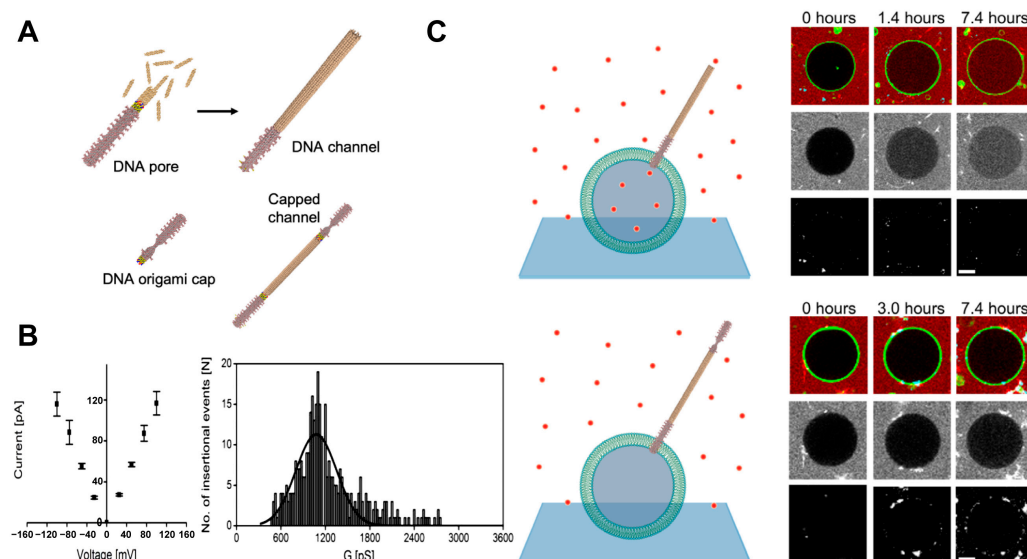


**Figure 4.** DNA tile-based transmembrane channels. (A) Schematic diagram of the channel structure. (B) Current-voltage relationship of the DNA tile-based transmembrane channels (left). Histogram of the conductance steps of the DNA tile-based transmembrane channels (right). The images in (A,B) were reproduced with permission from ref. [56], copyright 2022, bioRxiv. (C) Transport of dye molecules is hindered by DNA origami caps. The circles with green fluorescence in the figure refer to GUVs, and the red dots are small molecule dyes. Image reproduced with permission from ref. [57], copyright 2022, American Association for the Advancement of Science.

### 3.4. DNA Origami-Based Transmembrane Channels

DNA origami technology can be used for designing DNA-based channels; the shapes and sizes of the channels can be adjusted precisely, systematically, and abundantly [19]. DNA origami, proposed by Rothemund in 2006, is a relatively new method for DNA assembly. Based on the principle of complementary base pairing, by utilizing the structural characteristics of DNA molecules, the long DNA strands folded in specific regions are fixed by short strands to construct the expected structure [58]. Due to its simple experimental conditions and high assembly efficiency, DNA origami has become a popular technology

for constructing artificial DNA nanochannels. Artificial DNA nanochannels have been comprehensively designed concerning their pore size, length, and morphology characteristics.

Artificial DNA nanochannels can be exploited for size-dependent, selective transmembrane transport. The pore diameter is critical for the selective delivery of substances of different sizes. Transmembrane channels with large pore sizes are required for the transport of macromolecular substances. To this end, long DNA strands that are arranged longitudinally are initially used as basic units to construct channels, and the inner diameters of these channels are <9 nm [25–28]. A method of lateral assembly of DNA strands to form channels has been proposed; the same amount of DNA strands can be used to obtain artificial DNA nanochannels with a relatively large pore size (~35 nm) [29,30]. Inspired by the natural channel protein  $\alpha$ -hemolysin, Simmel et al. [25] have constructed a DNA nanochannel based on DNA origami technology. The channel consists of a tube that penetrates the membrane and a barrel cap on the periphery. The tube protrudes from the center of the barrel cap and features six DNA duplexes (Figure 5A), with the inner part of the tube acting as a transmembrane channel. The tube is approximately 2 nm in diameter and 42 nm in length. The brim of the barrel cap is set with 26 cholesterol molecules to mediate adherence of the channel to the membrane. The average ohmic conductance of this channel is  $0.87 \pm 0.15$  nS in a mixed solution containing KCl and MgCl<sub>2</sub>. DNA nanochannels with pore sizes larger than 2 nm have been designed, and the morphological design of large-pore-size channels is highly complex and diverse. In 2016, the first DNA nanochannel was reported with a large pore size and large conductance embedded in lipid membranes [26]. The channel has been designed as a funnel-shaped structure with three intercovering layers, and the pore size gradually increases from the inside to the outside; the morphology and function are similar to those of the natural protein biofilm channel (Figure 5B). An ionic current recording experiment shows that the conductivity of this channel reaches 30 nS. In addition, Howorka et al. [27] have designed a similar DNA nanochannel with an inner diameter of approximately 7.5 nm and a top opening of 22.5 nm (Figure 5C). This realized the transmembrane transport of enhanced green fluorescent protein (EGFP; 27 kDa) and showed an interception effect on rhodamine B-dextran (70 kDa). These channel walls consist of at most three biphasic layers, and the DNA nanochannels can be stable on the membrane.

The DNA nanochannels synthesized by Kjems et al. [28] have flaps to adjust the cholesterol exposure on demand (Figure 5D). The DNA channels are composed of a double-layer irregular hexagonal cylindrical DNA structure with 46 hydrophobic spots (17 on the walls and 29 on the flaps). Three programmable DNA lobes are on the three nonadjacent sides of the channel and connected approximately 12 nm from the bottom of the channel by a single-stranded DNA hinge. In the closed state, each flap is near the channel wall due to two stable strands that are complementary to the bottom single-strand portion of the channel. The flanking closure can protect the hydrophobic moiety from the aqueous environment and limit hydrophobicity-driven channel aggregation. When a key strand fully complementary to the single-stranded DNA is present around the channel, the flaps are opened and the cholesterol is exposed, thereby driving channel insertion into the membrane. Furthermore, Dekker et al. [29] have designed and assembled a DNA channel with a rigid octagonal ring structure. This channel is formed by folding 7560 base-long scaffold single strands and 240 individual oligonucleotide single strands, arranged in a  $4 \times 4$  duplex pattern (Figure 5E). A total of 32 cholesterol molecules are uniformly arranged on the surfaces of the channels. In addition, K<sub>10</sub>-PEG<sub>5K</sub> molecules are coated to stabilize the octagonal structure of the channels and prevent the aggregation of cholesterol-modified channels. The K<sub>10</sub>-PEG<sub>5K</sub> molecule consists of 10 positively charged lysine amino acids (K) linked to a short polyethylene glycol (PEG; 5 kDa). This channel has the largest inner diameter among the reported DNA-based transmembrane channels at 35 nm. Recently, a series of structurally concise DNA nanochannels with different pore sizes have been constructed by using bundled DNA duplex subunits [30]. The channel is designed with an outer membrane cap structure to define the overall pore shape and a barrel structure in the center for puncturing the membrane. Subunits are modularly arranged parallel to

the membrane to form pores of specific shapes, such as triangles, squares, pentagons, and hexagons (Figure 5F). Adjusting the number of duplex subunits can regulate the height and shape of the channel, and tuning the number of bases per subunit can regulate the pore size of the channel. The subunits of the cap are linked by short single-stranded (ss) DNA at the innermost double-stranded (ds) position. Furthermore, a short duplex of DNA is added between the double strands of the outermost subunit of the cap. This was conducted to prevent the cap from flipping and deviating from its designed shape.

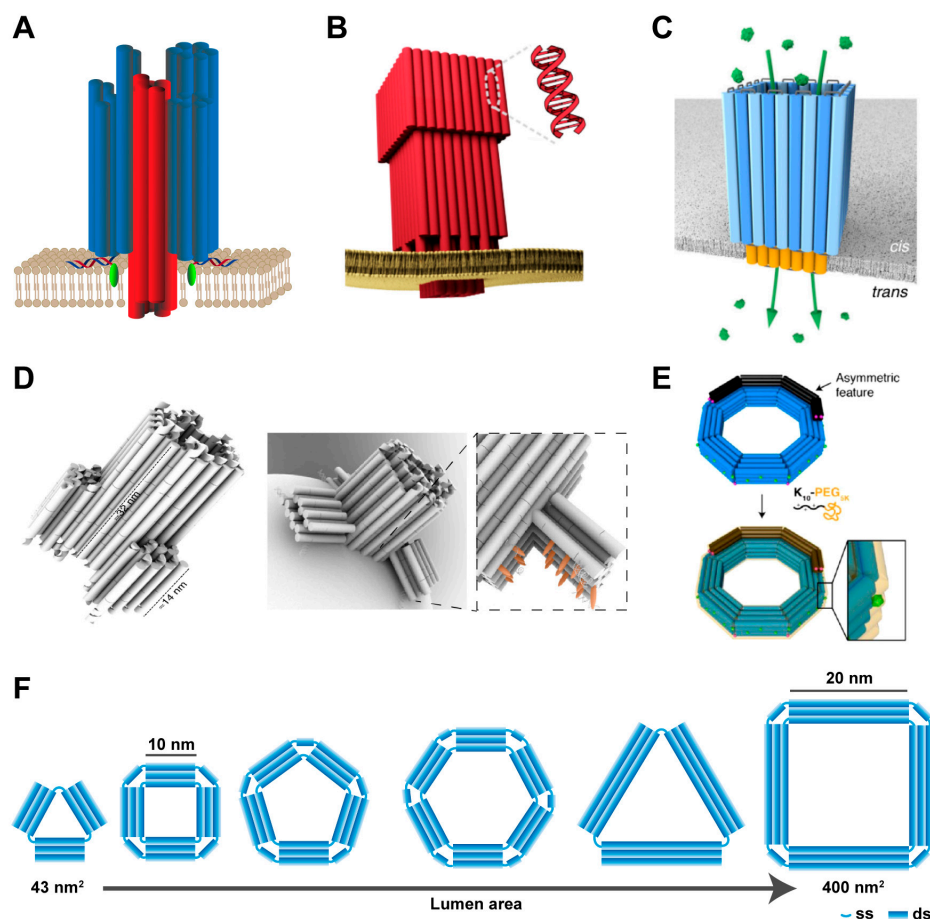


**Figure 5.** DNA origami-based transmembrane channels. (A–C) are schematic structures of various DNA origami transmembrane channels. (B) was reproduced with permission from ref. [26], copyright 2016, American Chemical Society. (C) was reproduced with permission from ref. [27], copyright 2019, Springer Nature. (D) Schematic representation of the DNA origami transmembrane channel with flanks in the closed (left) and open (right) states. Reprinted with permission from ref. [28], copyright 2019, Springer Nature. (E) Schematic diagram of the DNA origami transmembrane channel coated with  $K_{10}$ -PEG $_{5K}$  molecules. Reprinted with permission from ref. [29], copyright 2021, American Chemical Society. (F) Top view of the DNA nanochannels with different apertures and different shapes formed by the assembly of 10 nm or 20 nm subunits. The pore areas of DNA nanochannels with different polygonal shapes and sizes ranged from 43 nm<sup>2</sup> to 400 nm<sup>2</sup>.

### 3.5. Other DNA-Based Transmembrane Channels

G-quadruplex, a DNA duplex with unique ion transport properties, is utilized to design transmembrane channels. Depending on the hydrogen bond between the nitrogen and oxygen atoms of guanosine and the  $\pi$ - $\pi$  stacking between the bases, guanine (G)-rich DNA single strands can be deformed or aggregated to form a G-quadruplex structure with a central hole [59]. Moreover, the stability of the G-quadruplex depends heavily on certain cations, such as  $K^+$ ,  $Na^+$ ,  $NH_4^+$ , and  $Ca^{2+}$  [60]. Within the central channel, each ion is completely dehydrated and interacts with the guanine carbonyl  $O_6$  atom around

the pore (Figure 6A). This particular feature is reminiscent of the selectivity filters in  $K^+$  ion channel proteins first noted by Feigon et al. Because of this structural similarity, the G-quadruplex is a candidate for the design of artificial ion channels for selective transmembrane transport of  $K^+$  [61–63]. Dash et al. [33] have used telomere DNA to form a G-quadruplex and additionally modified lipophilic guanosine to construct an artificial potassium ion transmembrane transport carrier (Figure 6B). Liu et al. [35] have proposed a G-quadruplex consisting of single-stranded DNA modified with three lipophilic  $C_{12}$  spacers and cholesterol as an intelligent transmembrane channel to selectively transport  $K^+$  across the membrane.

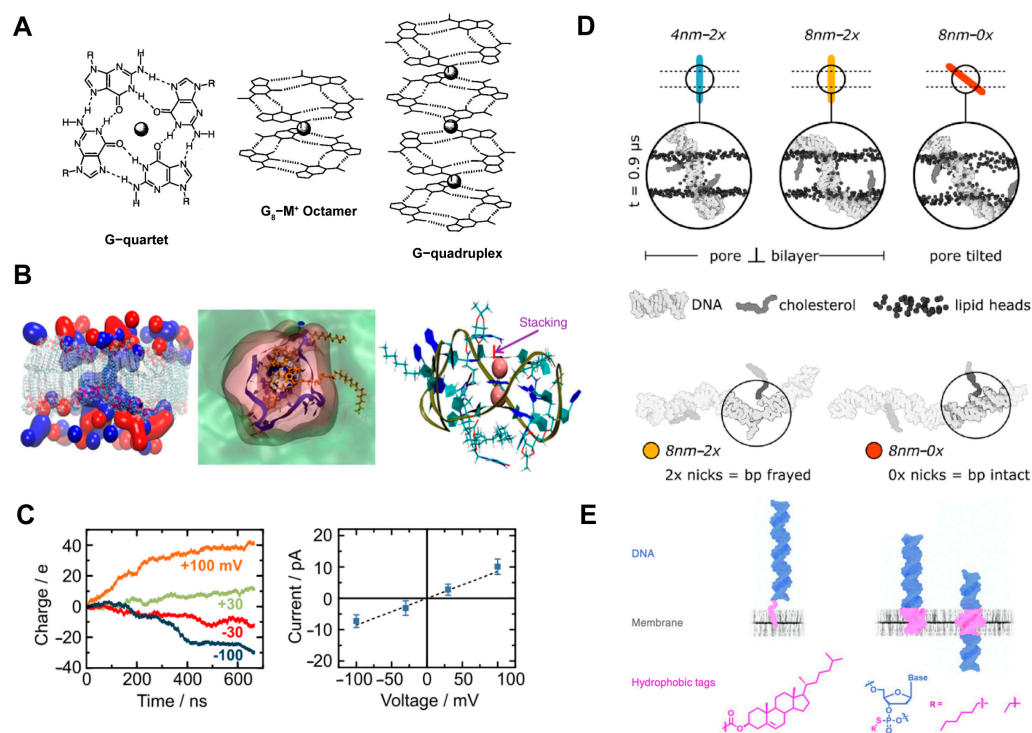


**Figure 6.** G-quadruplex or single DNA duplex-based artificial transmembrane channels. (A) Schematic representation of the structure of the G-quartet and G-quadruplex. Adapted with permission from ref. [59], copyright 2001, American Chemical Society. (B) Distribution of  $K^+$  (blue) and  $Cl^-$  (red) ions in a channel formed by lipophilic G-quadruplex (left). The middle is the top view of the transmembrane channel, containing the lipid layer (green), water pore (pink), and G-quadruplex (blue) modified by lipophilic guanidine (orange). The structure of the lipophilic G-quadruplex is given on the left. Image was adapted with permission from ref. [33], copyright 2020, Springer Nature. (C) Cumulative charge transmitted across the lipid bilayer and the current-voltage characteristics. Images were adapted with permission from ref. [64], copyright 2016, American Chemical Society. (D) Simulation of the interaction of DNA duplexes (cholesterol modification distance of 4 nm or 8 nm) with and without nicks with the phospholipid bilayer. Image was adapted with permission from ref. [65], copyright 2021, American Chemical Society. (E) Hydrophobic design of lipophilic DNA duplexes and their interactions with lipid bilayers. Image was adapted with permission from ref. [22], copyright 2021, American Chemical Society.

In addition, Keyser et al. [64] have constructed an artificial DNA nanochannel capable of ion conduction using a single long duplex (Figure 6C). MD simulations have shown that cholesterol modification leaves terminal base pairs of DNA structures with gaps, resulting in distortion when embedded in lipid bilayers (Figure 6D). The DNA nanostructure backbone can form stable conductive pores and be inserted into membranes at a higher efficiency than equivalent notched structures. In addition, the notation-free DNA structure can be designed to modulate its tilt orientation within the lipid bilayer. Reducing the degrees of

freedom of DNA conformation and adjusting the positions of hydrophobic modifications can control the function of this structure as a synthetic ion channel well (Figure 6E) [22,65].

#### 4. Artificial Transmembrane Channels for Biosensing and Biomedical Applications

DNA-based artificial channels on the cell membrane have been widely used for biosensors and biomedicine. For example, they are used for DNA strand translocation [25,34], ions ( $K^+$ ,  $Ca^{2+}$ , and  $Pb^{2+}$ ) [31,33,35,42], small molecules (dyes and drugs) [23,66], and large molecules (EGFP, GFP, IgG, and dextran) [27–30,67] transmembrane transport (Table 1). Artificial DNA channels with gates can modulate material transport under specific conditions. These channels provide tools for molecular sensing, artificial cell design, and cell communication, achieving controlled transmembrane transport to cells and regulating cell behavior.

##### 4.1. DNA-Based Transmembrane Channels for Biosensors

###### 4.1.1. Single-Molecule Nanochannel Sensors

Transmembrane DNA channels have been proposed for use as single-molecule nanochannel sensors. In biomimetic sensing experiments, the translocation of analyte molecules leads to current changes in membrane pores and the duration and depth, which are related to the charges and sizes of the analytes. For example, DNA channels designed by Simmel et al. [25] have been used for single-molecule sensing. A stable baseline current is detected on the lipid membrane containing the artificial DNA channels. The additions of the hairpin molecules at the beginning and ~30 min later show transient current blocking, in which the applied voltage can capture, decompress, and translocate the hairpin structure (Figure 7A). Another set of experiments shows that lengthening the tail of the quadruplex increases current blocking. The average current blockades of the quadruplexes with single-stranded tails consisting of 60 and 125 thymidines (Q-T60, Q-T125) are  $\Delta I_{Q-T60} = 5.6 \pm 1.0$  pA and  $\Delta I_{Q-T125} = 15.3 \pm 2.3$  pA, respectively (Figure 7B). Thus, similar to biological pores, artificial DNA nanochannels can be used as sensing devices to distinguish analyte molecules by studying their translocation properties. The T-pore designed by Simmel et al. allows the translocation of double-stranded DNA (dsDNA) molecules (Figure 7C) [34]. As the transmembrane voltage increases, the velocity of the molecule and the frequency of translocation events increase (Figure 7D), while the dwell time within the channel decreases.

DNA channels have been used to identify and detect proteins. Howorka et al. [30] have used DNA nanochannels to identify human SARS-CoV-2 antibodies with a handheld MinION kit (originally intended for portable DNA sequencing). The cognate receptor SARS-CoV-2 spike protein attaches to an adaptor oligonucleotide on the inner wall of the Tri-20 channel through an irreversible metal chelate bridge (Tri-20-spike). In the presence of a human SARS-CoV-2 antibody, the conductivity of Tri-20-spike is significantly reduced, and the average dwell time of the antibody is  $1.7 \pm 8.6$  s.

###### 4.1.2. Ligand-Gated Artificial Transmembrane Channels

The DNA-based artificial transmembrane channels are mostly hollow tubes with openings. Voltage gating is observed in almost all DNA nanochannels, but channels with additional gates are highly flexible and controllable [68]. Therefore, the design of artificial channels with ligand-gated opening or closing properties has become the focus of research. The reported artificial DNA nanochannels with gates can specifically recognize key strands. Howorka et al. [66] built an artificial channel with a gate that can be opened with a key strand. The lock of the channel is tightly bound to the entrance by hybridizing with two docking sites to form a spiral bundle across the channel opening. The docking site is formed by the extension of two duplex support rods in opposite positions. The key can be hybridized with the lock strand to remove it, leaving the channel open. After being modified by cholesterol, such channels can be used to regulate the flow of small organic molecules (including many important drug compounds), which have broad application

prospects in biomedicine. A large square DNA origami nanochannel with 0 (open state), 2 (semiclosed state), or 4 (closed state) strips of DNA lock can block the molecular penetration mechanism, improving the selectivity of molecular penetration of artificial DNA nanochannels (Figure 8A) [69].

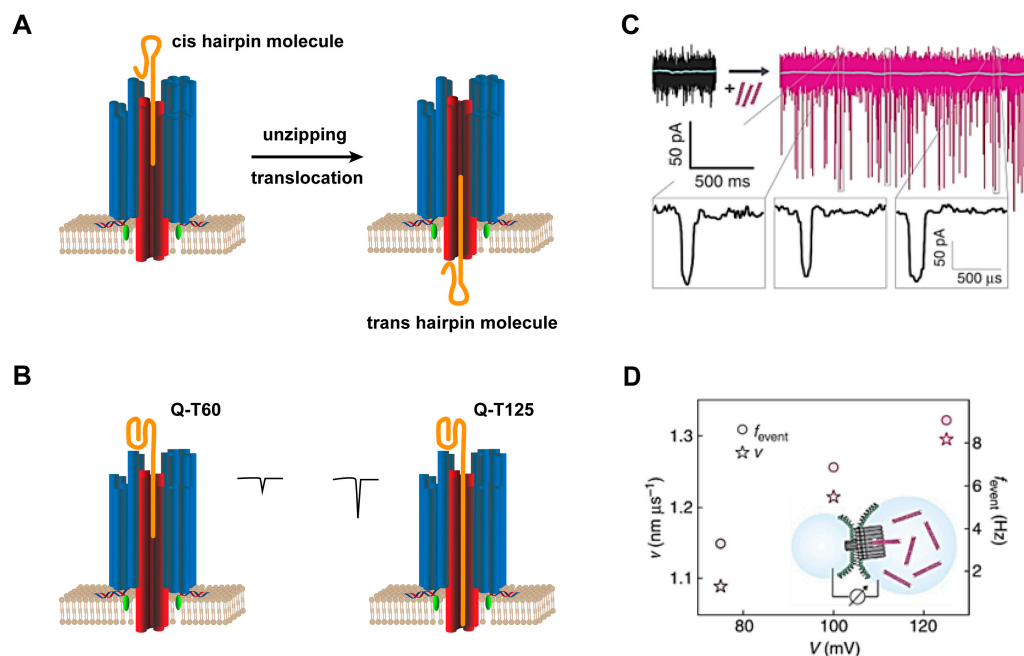


**Figure 7.** Single-molecule nanochannel sensors. (A) Schematic diagram of DNA hairpin strand capture and translocation on transmembrane DNA channels. (B) Current blockade of DNA quadruplexes with different tail lengths on transmembrane DNA channels. (C) Current on the transmembrane channel in the absence/presence (left/right) of the analyte. The bottom shows three current signals at the time of dsDNA translocation. (D) dsDNA translocation velocities and event frequencies detected at 75, 100, and 125 mV. The images in (C,D) were reproduced with permission from ref. [34], copyright 2016, Springer Nature.

To exploit the potential of DNA-based artificial channels as real-time smart sensing devices, Kjems et al. [28] have designed a bolt on the inside of the channel. PEG is used as a plug that connects the toehold sequence with 8 nucleotides to partially block the gateway (Figure 8B) and allows small molecules (ATTO 655) to pass through (Figure 8C). The unplugged strand is combined with the toehold-mediated strand to remove PEG so that the macromolecular material (dTMR-40k) can pass through the artificial DNA nanochannel. Another reversible gated protein transport membrane channel is constructed based on a horizontal routing DNA origami design strategy with a large pore size of 20.4 nm (Figure 8D) [67]. The passageway opening is designed with a square cover, one side of which is attached to the cap by a flexure hinge. The other side of the cap carries two single strands that can be hybridized with the two single strands on the cap to form a complete double lock. Two key strands are added to the system to open the lock and lid. The lid is switched back to its closed state with a single-strand reverse key pair. This channel allows the precisely timed transport of folded proteins across the membrane. A potential disadvantage of covered channels is that they may leak when closed or when inserted in a double layer. Howorka et al. [70] designed a channel formed by the assembly of two subunits after being triggered by ligands on the membrane. The whole channel consists of two parts, component A and component B, each of which contains a complete duplex and two single strands (Figure 8E). The complementary binding of single strands on the two components allows channel formation. Adding a key unlocks the locks on both components and restores their binding ability. Each component carries one cholesterol, and after the channel forms, the cholesterol is on the opposite side of the channel wall.

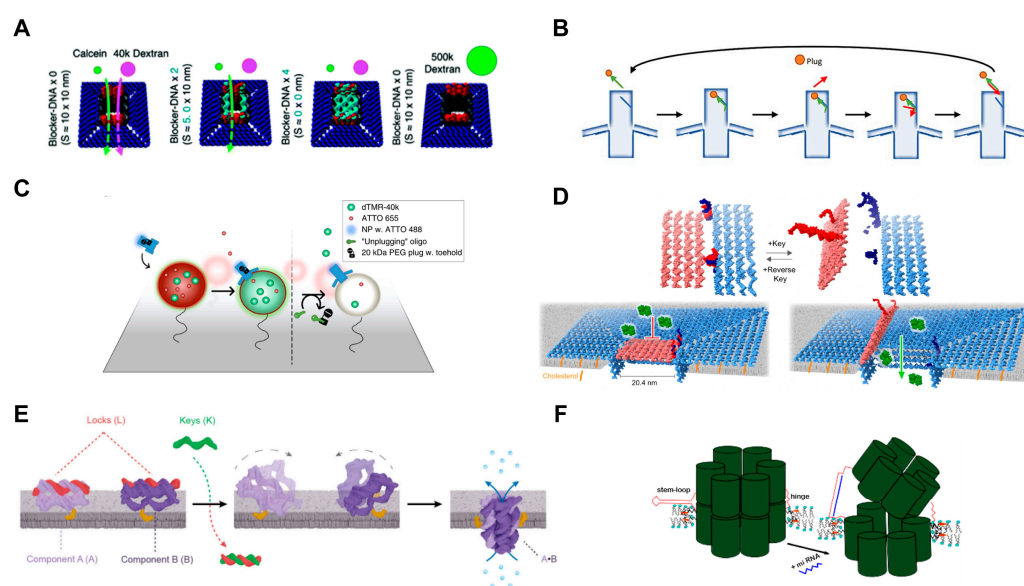


**Figure 8.** Ligand-gated DNA-based artificial transmembrane channels. (A) Schematic representation of the passage/blockage of the dye molecule by the blocker DNA. From left to right are 0, 2, and 4 blocker DNA channels. The channel is designed with a pore size of 10 nm, and it does not allow the passage of 500 k dextran (far right). Image was adapted with permission from ref. [69], copyright 2021, Royal Society of Chemistry. (B) Schematic representation of an artificial transmembrane DNA nanochannel with a bolt (blue) recognizing an unplugging oligo (red arrow). In the figure, the orange plug is PEG, and the green arrow is the toehold strand. (C) Schematic diagram of an artificial transmembrane DNA channel with a bolt before (left) and after (right) adding an unplugging oligo. (B,C) were adapted with permission from ref. [28], copyright 2019, Springer Nature. (D) A large DNA nanochannel (blue) with a reversible gate (pink). The mechanism of opening and closing by a key and the reverse key is designed. Two sets of locks (red and dark blue) are located on the lid and the cap. Adapted with permission from ref. [67], copyright 2022, Springer Nature. (E) Schematic diagram of the formation of a DNA membrane channel in which the key strands trigger assembly. Adapted with permission from ref. [70], copyright 2022, American Chemical Society. (F) Schematic representation of DNA transmembrane channels disrupted by tension dependent on the duplex. Adapted with permission from ref. [71], copyright 2022, Wiley-VCH.

Since the DNA duplex is quite stiff and has a persistent length, Elezgaray et al. [72] have designed a DNA channel with two conducting states: closed (low current) and open (high current). The transition of the channel from closed to open is triggered by ssDNA. When the lock at the entrance of the 6-HB DNA channel binds to the complementary strand, the resulting duplex exerts tension on the channel structure, locally widening the pore size. In 2022, Elezgaray et al. [71] designed another channel that relies on the tension of the duplex to switch in the vertical directions, proposing that this design can detect short oligonucleotide sequences (Figure 8F).

#### 4.1.3. Environmental Stimuli-Responsive Artificial Transmembrane Channels

Environmental stimuli-responsive artificial channels have been designed to be sensitive to temperature [73], light [74–76], and ions [77]. The temperature-responsive DNA channel constructed by Howorka et al. [73] has two main parts: a transmembrane barrel-shaped nanotube and a reversibly sealed lid at the top. Biphasic segments 1–4 are designed between the channel and the lid, with a designed melting temperature of approximately 40 °C for segments 2–4 and 62.8 °C for segment 1 (Figure 9A). The lid is hybridized to the two elongated rings of the channel at room temperature to block the mass influx. Temperatures higher than 40 °C selectively separate the lid from loop segments 2–4 to allow the cap to open. By adjusting the temperature, the lid of this channel can achieve reversible on/off functionality. Azobenzene is a reversible cis-trans photoisomerization switchable

compound. The conversion of azobenzene from the *trans* isomer to the *cis* isomer can be triggered by light irradiation with a wavelength  $\lambda < 400$  nm, and the reverse effect can be achieved by illumination at  $\lambda > 400$  nm [74]. The *cis-trans* isomerization of azobenzene can adjust the on/off state of the channel. Howorka et al. proposed a 6-HB-based DNA channel, and *cis*-azobenzene corresponded to the closed state (Figure 9B) [75]. Liu et al. designed a DNA transmembrane channel based on a lipophilic G-quadruplex, in which *cis*-azobenzene causes G-rich DNA strands to assemble into channels for the transmembrane transport of ions [76]. The ion-dependent G-quadruplex channel can be utilized for selective ion transport [77]. Guanine-rich lipophilic ssDNA can form different G-quadruplex isomers with different metal cations [78,79]. Therefore, a biomimetic ion channel is designed based on the G-quadruplex for conformation-dependent selective ion transport to membranes. Specifically, the  $\text{Pb}^{2+}$ -stable antiparallel conformation G-quadruplex (apG4) preferentially mediates the transmembrane transport of  $\text{Pb}^{2+}$ , while the  $\text{K}^+$ -stable parallel conformation G-quadruplex (pG4) promotes the highly selective transport of  $\text{K}^+$  (Figure 9C).

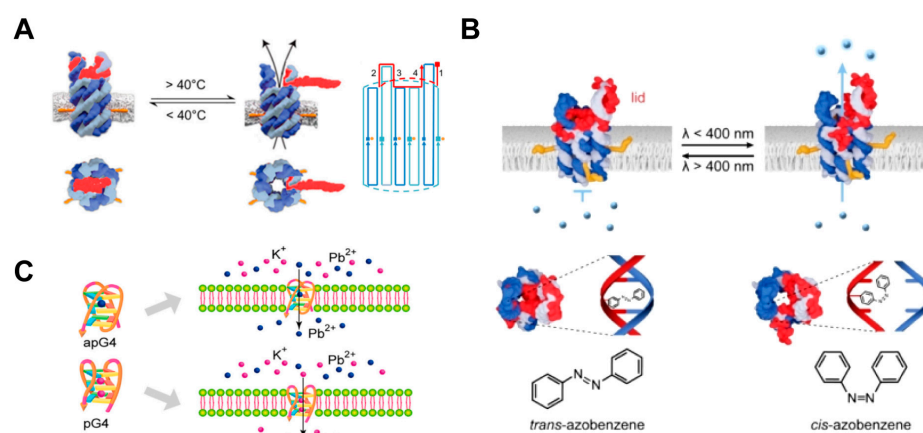


**Figure 9.** Environmental stimuli-responsive artificial transmembrane channels. (A–C) are the channels that depend on temperature, light, and ion recovery transport functions, respectively. (A) was adapted with permission from ref. [73], copyright 2019, American Chemical Society. (B) was adapted with permission from ref. [75], copyright 2022, John Wiley and Sons. (C) was adapted with permission from ref. [77], copyright 2020, American Chemical Society.

#### 4.2. DNA-Based Transmembrane Channels for Biomedical Applications

##### 4.2.1. Cell Mimics for Transmembrane Transport

Artificial DNA nanochannels can serve as synthetic cell membrane components to mimic transmembrane transport. Currently, the transport selectivity of DNA transmembrane channels is largely determined by their pore size. The molecules or ions smaller than their pore size are easily mass-transportable. Meanwhile, the negatively charged DNA ion channel has a poor transport capacity for negatively charged ions. Artificial DNA transmembrane channels with large pores have been proposed for the transmembrane transport of drugs, immune proteins, and so on. In 2016, Howorka et al. [80] were inspired by organelles to create synthetic hybrid nanocontainers composed of polymersomes and DNA nanochannels (Figure 10A). Nanocontainers exhibit size-dependent permeability. These containers enable the transport of the enzyme substrate across the membrane while retaining the relatively large enzyme inside the container. These nanodevices can be used to simulate the site where biocatalytic reactions occur. The 6-HB DNA nanochannels modified with three cholesterol molecules on this container mimic the protein channels in biofilms and enable specific substance transport (Figure 10B). Tan et al. [42] have constructed an artificial signal transduction network using two synthetic cell communities formed by vesicles containing different DNA structures modified with cholesterol (Figure 10C). This system is used to simulate cell-to-cell communication, in which giant membrane vesicles derived from living cells are used as cell models. This signal transduction system consists

of two groups of giant membrane vesicles, one as a stimulator and one as a receptor for signal actuation. The stimulation group is modified with a DNA triangular prism stimulator (TP<sub>B</sub>). The receptor group contains the DNA triangular prism receptor (TP<sub>A</sub>) and transmembrane channel. The transmembrane channel is designed with a lock strand that closes the mass entrance. When a toehold strand displacement reaction is performed with a foreign complementary key strand, the lock strand is released from the transmembrane channel to reopen the channel. In this system, the key is derived from TP<sub>A</sub>. When the two groups of artificial cells approach each other, TP<sub>B</sub> combines with TP<sub>A</sub>. Afterward, the key strand originally on the TP<sub>A</sub> breaks away to recombine with the lock strand on the wireframe, thus opening the channel. Then, extramembranous Ca<sup>2+</sup> flows into the receptor vesicles, allowing calcein, which is encapsulated inside the vesicle, to respond. The DNA nanochannels exhibit high efficiency, accuracy, and programmability as signal receivers and actuators in this system. They make it possible to precisely manipulate signal transduction systems, address the high-order complexity of cell simulations well, regulate the behaviors of natural cells, and control the release of therapeutic drugs at disease sites.

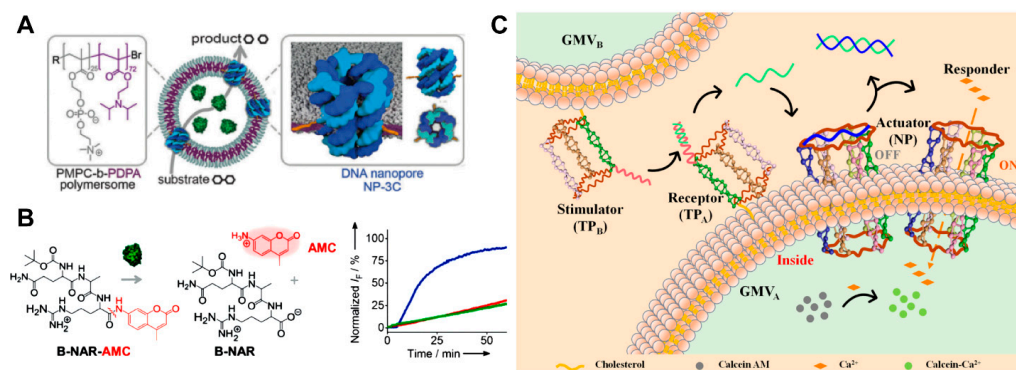


**Figure 10.** Cell mimics for transmembrane transport. (A) Nanocontainers formed by the self-assembly of PMPC-b-PDPA polymersomes coated with enzymes (green). DNA nanochannels (blue) are embedded in the membrane to allow the substrates and products of the enzyme to shuttle across the membrane. (B) Schematic diagram of the structure of the trypsin-hydrolyzed substrate peptide and the results of fluorescence detection. The fluorescence kinetics curves of the loaded enzyme hydrolyzed peptide with the addition of three (blue) or zero (red) cholesterol nanochannels or without the addition of a nanochannel (green). (A,B) were adapted with permission from ref. [80], copyright 2016, John Wiley and Sons. (C) Design of the artificial signal transduction system based on DNA triangular prisms, DNA hexagon prism nanochannels, and giant membrane vesicles. Reprinted with permission from ref. [42], copyright 2021, American Chemical Society.

#### 4.2.2. Transmembrane Channels for Cell Death

Artificial transmembrane channels can selectively control ion transport across biological membranes, and artificial channels can disrupt cellular homeostasis of cell death. Howorka et al. [81] designed a DNA channel with a highly hydrophobic 2-nm band composed of ethyl phosphorothioate (EP) at one end, which can penetrate the cell membrane and cause cell cytotoxicity. Tan et al. [82] have found that phosphorothioate (PPT)-modified DNA nanochannels can be spontaneously inserted into the cell membrane (Figure 11A), and they can transport ions and antitumor drugs to neurons and cancer cells, respectively. It has been proposed that their potency can be improved by specifically binding target cancer cells. Loading chemical toxins, such as doxorubicin, with DNA insertion enhances chemical toxicity. In 2019, Zhang et al. [83] proposed a design for the controlled transfer of DNA nanochannels to the plasma membrane. This approach enhances the insertion of DNA nanochannels, inducing membrane depolarization and pyroptosis-like cell death. 3D tumor spheroid experiments show that this process can induce tumor cell death and significantly inhibit tumor growth. A series of experimental results have shown that this device exhibits

antitumor ability. It induces a host antitumor immune response by promoting antigen presentation and activating T cells and natural killer cells (Figure 11B).

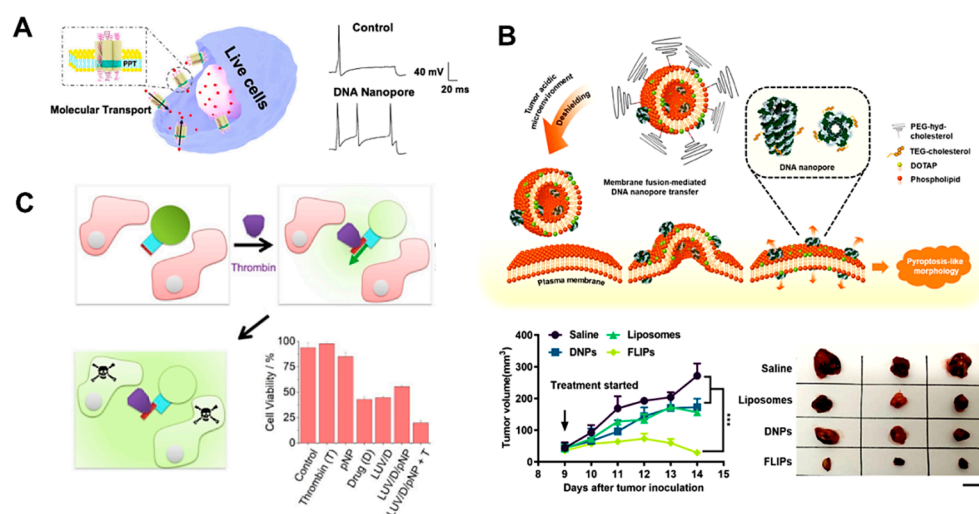


**Figure 11.** Transmembrane channels for cell killing. (A) Schematic illustration of DNA nanochannels embedded in cell membranes to deliver drugs. Dorsal root ganglia (DRG) neurons with channels inserted had more evoked action digits than those without channels. Reproduced with permission from ref. [82], copyright 2020, American Chemical Society. (B) Illustration of the transfer of nanochannels from vesicles to the plasma membrane. In the acidic tumor microenvironment, vesicles with DNA nanochannels can be activated to fuse with cell membranes. DNA nanochannels were successfully transferred to the plasma membrane after fusion. Inhibition of tumor growth was detected 9 days after vesicular DNA nanochannel treatment in C57BL/6 mice bearing Hepa1-6 xenografts. Reproduced with permission from ref. [83], copyright 2020, American Chemical Society. (C) Schematic representation of protein-triggered DNA nanochannels opening on vesicles to release drugs for cell killing. The bottom right corner shows the survival statistics of HeLa cells treated with different substances for 3 days. Reproduced with permission from ref. [84], copyright 2020, John Wiley and Sons.

Artificial transmembrane channels with large cavities can be exploited for the controlled transport of chemical drugs for cell behavior modulation or cell death. For example, DNA nanochannels with protein-controlled gates have been successfully applied to the off-on transport of topotecans [84]. The DNA-based artificial channels are inserted into GUVs filled with 3  $\mu$ M topotecan. Topotecan is a clinically used cytotoxic agent with activity against cervical cancer. In the experiment, tri-component vesicles are first added to HeLa cervical cancer cells. The results show that cytotoxic drugs (D) are released to reduce cell viability to  $20 \pm 2\%$  when both channels and thrombin (T) are present (Figure 11C). To date, artificial nanochannels for tumor cell killing are mostly nontargeted, and their actual application endangers healthy cells to varying degrees [85]. Depending on the diversity of DNA nanostructures, it is feasible and necessary to improve the targeting ability of DNA nanochannels in the application process. If the designed channel has a target recognition function, it can reduce damage to normal cells, improve the binding rate between the channel and target cells, and enhance the cell death effect [86,87].

**Table 1.** Design and applications of DNA-based artificial transmembrane channels.

Type	Pore Size and Length (nm)	Hydrophobic Modification	Applications	Refs.
Cubical	7; 7	4 or 8 cholesterol on the two opposite faces of the cube	Dye molecular transmembrane transport	[23]
Hexagonal prism	-	4 cholesterol	Transport Ca <sup>2+</sup> across the membrane as a part of the artificial signal transduction system	[42]
6-helix bundle	2; -	Ethyl-phosphorothioate	1. K <sup>+</sup> transmembrane transport 2. Selectively cytotoxic to cervical cancer cells 3. Transport ions and antitumor drugs (DOX) to neurons and cancer cells, respectively	[31,44,45]
4-helix bundle	0.8; -	2 cholesterol	Ion conduction	[21,49]
Micron-length	7.3; Micron	12 cholesterol	Leakless end-to-end transport of carboxytetramethyl-rhodamine	[57]
Capped	2; 47	26 cholesterol at the underside of the subunits' caps	DNA hairpin and guanine quadruplex translocation	[25]
Funnel-shaped	6; 54	19 cholesterol	Large ionic conductance	[26]
Protein-conductive	7.5; 46	24 cholesterol	Proteins transmembrane transport	[27]
Large size-selective	9; 32	18 cholesterol and 28 palmitoyls at the terminal of channel and the underside of the flap	1. Size-specific cargo translocation 2. Real-time direct observation of sensing of an oligonucleotide unplugging strand	[28]
Ultrawide	35; 10	32 cholesterol	Transmembrane transport of green fluorescent protein (GFP)	[29]
Highly shape- and size-tunable	8.66~20; -	Underside of the subunits' caps (10 cholesterol on each 10-nm subunit, 15 cholesterol on each 20-nm subunit)	1. IgG sensing 2. Human SARS-CoV-2 anti-bodies detection	[30]
G-quadruplex and liponucleoside	-	Lipophilic guanosine binds to the G-quadruplex with a 3:1 stoichiometry	The transport of K <sup>+</sup> across CHO and K-562 cell membranes	[33]
Lipophilic G-quadruplex	-	3 C <sub>12</sub> spacers and 1 cholesterol on each strand	Switchable K <sup>+</sup> transport	[35]
Single-duplex	-	6 tetraphenyl porphyrins	Ion conduction	[64]
T-like	3.7; 27	57 tocopherols at the bottom of the double-layered plate	1. DNA translocation 2. Molecular transmembrane transport	[34]
Ligand-controlled	-; 9.0 ± 1.5	3 cholesterol	Controlled DNA-triggered and charge-selective release of small-molecule cargo (sulfo-rhodamine B, SRB) from a reservoir	[66]
Large, square	10; 24	47 strands at the bottom of the nanopore, complementary to the anchor DNA on the phospholipid membrane	Selective transmembrane transport of molecules with different sizes (calcein, 40 k or 500 k dextran)	[69]
Reversibly gated	20.4; -	64 cholesterol	1. Dye molecular (Atto633) transmembrane transport 2. Dynamically controlled cargo (Atto633 and GFP) transport across the lipid bilayer	[67]
Trigger-assembled	0.8; 7.5	One cholesterol per component (A or B)	Ion conduction	[70]

Table 1. Cont.

Type	Pore Size and Length (nm)	Hydrophobic Modification	Applications	Refs.
Tensegrity driven	$\sim 4 \pm 0.2$	4 cholesterol driven channels inserted into the membrane and 2 cholesterol grafted at the ends of two strands facing each other on one side of the barrel	Controlled transmembrane transport of SRB	[72]
Temperature-gated	2; -	4 cholesterol	Permitted temperature-controlled transport of molecular cargo (SRB) across the bilayer	[73]
Light-triggered synthetic	2; 12.5	4 cholesterol	Light-gated small-molecule (SRB) transport	[75]
8-helix bundle	4; 14	4 TEG-cholesterols	1. Depolarized plasma membrane to induce pyroptosis 2. Inhibited tumor growth	[83]
Protein-controlled	Molecular gate approximately $13 \text{ nm} \times 5 \text{ nm} \times 5 \text{ nm}$	4 cholesterol	1. Controlled transport of molecular cargo (SRB) across lipid bilayers 2. Released cytotoxic drug (topotecan) for cell killing	[84]

## 5. Conclusions and Perspectives

In this review, we describe the design of DNA-based artificial transmembrane channels and their applications in biosensing and biomedicine. Different kinds of artificial transmembrane channels have been developed based on DNA wireframes, DNA helix bundles, DNA tiles, and DNA origami assembly technologies. However, there are still many challenges in the artificial transmembrane DNA nanochannels reported herein for applications. For example, there is some degree of leakage while transmitting material. For example, some positively charged dyes could leak out due to their membrane permeability. Additionally, the channel or gating structure is unstable, and aggregation of channels due to hydrophobic modifications still occurs. Thickening the channel wall or coating it with other polymers can effectively reduce material leakage while stabilizing the channel structure [51]. The controllable assembly of DNA nanochannels prevents the material from leaking in advance; the assembly can be stimulated at a specific time to combine the parts to form channels [72]. The main solution to the problem of channel aggregation is to adjust the type, number, and position of hydrophobic modification groups [25,34]. Designing unique channel structures or aiding surfactants are special approaches that have been proposed [28,29,88].

Previous studies have focused on the biomedical applications of artificial transmembrane channels. However, the mode of action of DNA nanochannels is relatively simple and only depends on the toxicity of the channel to cells or the transmembrane delivery of drugs to kill tumor cells. There is room for improvement in the ability to transport ions, proteins, or drugs across membranes in a form similar to passive transport. Enriching the function of DNA nanochannels, such as enabling the same channel to transport different substances in unique states, may enhance their ability to induce apoptosis [67]. The proposed optimal design is to endow DNA nanochannels with functions similar to ion pumps at the cell membrane or channels that enable active transport, moving the material uphill against a concentration gradient [89,90]. The DNA duplex rotates in one direction at a rate of billions of revolutions per minute under the action of an electric field, and the direction of rotation is determined by the chirality of the duplex [91]. It is challenging to design energy-driven active transport based on the DNA transmembrane channels. Recently, Ma et al. fabricated a bionic micropump for active transmembrane drug delivery by immobilizing urease on the surface of silica-based microtubules [92]. The above results provide evidence for the possibility of the active transport function of DNA nanochannels.

The biomedical applications of transmembrane channels are not limited to cancer therapy [93]. DNA nanochannels with ion transport functions may contribute to the

treatment of ion channel diseases [94]. The vast majority of ion channel diseases are associated with genetic mutations that determine the performance of ion channels [95]. The mutations are partly caused by other diseases that damage the membrane channel synthesis pathway or function [96]. In the future, artificial transmembrane channels are expected to be used as biomimetic membrane channels for the controlled transport of substances in the physiological environment to alleviate the symptoms and treatment effects caused by ion channel diseases. We will explore complex physiological operation pathways with artificial transmembrane channels, leading to further research on disease treatment and biomedical applications.

**Author Contributions:** Conceptualization, W.X., H.C. and J.L.; investigation, Y.L.; resources, H.C. and S.L.; writing—original draft preparation, W.X.; writing—review and editing, K.W. and J.L. All authors have read and agreed to the published version of the manuscript.

**Funding:** The authors gratefully acknowledge the financial support of the National Natural Science Foundation of China (22377025 and 22177032) and the Natural Science Foundation in Hunan Province (2022RC3047, 2021JJ10013, and 2022JJ40049).

**Institutional Review Board Statement:** Not applicable.

**Informed Consent Statement:** Not applicable.

**Data Availability Statement:** Not applicable.

**Conflicts of Interest:** The authors declare no conflict of interest.

## References

1. Shen, H.; Wang, Y.; Wang, J.; Li, Z.; Yuan, Q. Emerging Biomimetic Applications of DNA Nanotechnology. *ACS Appl. Mater. Interfaces* **2019**, *11*, 13859–13873. [[CrossRef](#)] [[PubMed](#)]
2. Shen, Q.; Xiong, Q.; Zhou, K.; Feng, Q.; Liu, L.; Tian, T.; Wu, C.; Xiong, Y.; Melia, T.J.; Lusk, C.P.; et al. Functionalized DNA-Origami-Protein Nanopores Generate Large Transmembrane Channels with Programmable Size-Selectivity. *J. Am. Chem. Soc.* **2022**, *145*, 1292–1300. [[CrossRef](#)]
3. Jiang, X.; Wang, L.; Liu, S.; Li, F.; Liu, J. Bioinspired artificial nanochannels: Construction and application. *Mater. Chem. Front.* **2021**, *5*, 1610–1631. [[CrossRef](#)]
4. Pugh, G.C.; Burns, J.R.; Howorka, S. Comparing proteins and nucleic acids for next-generation biomolecular engineering. *Nat. Rev. Chem.* **2018**, *2*, 113–130. [[CrossRef](#)]
5. Luo, Y.; Zhu, C.; Zhang, T.; Yan, T.; Liu, J. Self-assembled Supramolecular Artificial Transmembrane Ion Channels: Recent Progress and Application. *Chem. Res. Chin. Univ.* **2023**, *39*, 3–12. [[CrossRef](#)]
6. Langecker, M.; Arnaut, V.; List, J.; Simmel, F.C. DNA nanostructures interacting with lipid bilayer membranes. *Acc. Chem. Res.* **2014**, *47*, 1807–1815. [[CrossRef](#)] [[PubMed](#)]
7. Seeman, N.C.; Sleiman, H.F. DNA nanotechnology. *Nat. Rev. Mater.* **2017**, *3*, 17068. [[CrossRef](#)]
8. Ramezani, H.; Dietz, H. Building machines with DNA molecules. *Nat. Rev. Genet.* **2020**, *21*, 5–26. [[CrossRef](#)]
9. Suzuki, Y.; Endo, M.; Sugiyama, H. Mimicking Membrane-Related Biological Events by DNA Origami Nanotechnology. *ACS Nano* **2015**, *9*, 3418–3420. [[CrossRef](#)]
10. Wang, D.; Zhang, Y.; Liu, D. DNA nanochannels. *F1000Res* **2017**, *6*, 503. [[CrossRef](#)]
11. Wu, N.; Chen, F.; Zhao, Y.; Yu, X.; Wei, J.; Zhao, Y. Functional and Biomimetic DNA Nanostructures on Lipid Membranes. *Langmuir* **2018**, *34*, 14721–14730. [[CrossRef](#)] [[PubMed](#)]
12. Yin, P.; Hariadi, R.F.; Sahu, S.; Choi, H.M.T.; Park, S.H.; LaBean, T.H.; Reif, J.H. Programming DNA Tube Circumferences. *Science* **2008**, *321*, 824–826. [[CrossRef](#)] [[PubMed](#)]
13. Frykholm, K.; Muller, V.; KK, S.; Dorfman, K.D.; Westerlund, F. DNA in nanochannels: Theory and applications. *Q. Rev. Biophys.* **2022**, *55*, e12. [[CrossRef](#)] [[PubMed](#)]
14. Lanphere, C.; Offenbartl-Stiegert, D.; Dorey, A.; Pugh, G.; Georgiou, E.; Xing, Y.; Burns, J.R.; Howorka, S. Design, assembly, and characterization of membrane-spanning DNA nanopores. *Nat. Protoc.* **2021**, *16*, 86–130. [[CrossRef](#)]
15. Liu, X.; Zhao, Y.; Liu, P.; Wang, L.; Lin, J.; Fan, C. Biomimetic DNA Nanotubes: Nanoscale Channel Design and Applications. *Angew. Chem. Int. Ed. Engl.* **2019**, *58*, 8996–9011. [[CrossRef](#)] [[PubMed](#)]
16. Ma, Q.; Chen, L.; Gao, P.; Xia, F. Solid-state nanopore/channels meet DNA nanotechnology. *Matter* **2023**, *6*, 373–396. [[CrossRef](#)]
17. Gopfrich, K.; Ohmann, A.; Keyser, U.F. Design and Assembly of Membrane-Spanning DNA Nanopores. *Methods Mol. Biol.* **2021**, *2186*, 33–48.
18. Zhao, N.; Chen, Y.; Chen, G.; Xiao, Z. Artificial Cells Based on DNA Nanotechnology. *ACS Appl. Bio Mater.* **2020**, *3*, 3928–3934. [[CrossRef](#)]

19. Niranjana, D.N.; Thiyagarajan, D.; Bhatia, D. DNA Origami in the Quest for Membrane Piercing. *Chem. Asian. J.* **2022**, *17*, e202200591. [[CrossRef](#)]
20. Chen, J.; Seeman, N.C. Synthesis from DNA of a molecule with the connectivity of a cube. *Nature* **1991**, *350*, 631–633. [[CrossRef](#)]
21. Ohmann, A.; Li, C.Y.; Maffeo, C.; Nahas, K.A.; Baumann, K.N.; Gopfrich, K.; Yoo, J.; Keyser, U.F.; Aksimentiev, A. A synthetic enzyme built from DNA flips  $10^7$  lipids per second in biological membranes. *Nat. Commun.* **2018**, *9*, 2426. [[CrossRef](#)] [[PubMed](#)]
22. Jones, S.F.; Joshi, H.; Terry, S.J.; Burns, J.R.; Aksimentiev, A.; Eggert, U.S.; Howorka, S. Hydrophobic Interactions between DNA Duplexes and Synthetic and Biological Membranes. *J. Am. Chem. Soc.* **2021**, *143*, 8305–8313. [[CrossRef](#)] [[PubMed](#)]
23. Chidchob, P.; Offenbartl-Stiegert, D.; McCarthy, D.; Luo, X.; Li, J.; Howorka, S.; Sleiman, H.F. Spatial Presentation of Cholesterol Units on a DNA Cube as a Determinant of Membrane Protein-Mimicking Functions. *J. Am. Chem. Soc.* **2018**, *141*, 1100–1108. [[CrossRef](#)] [[PubMed](#)]
24. Burns, J.R.; Howorka, S. Defined Bilayer Interactions of DNA Nanopores Revealed with a Nuclease-Based Nanoprobe Strategy. *ACS Nano* **2018**, *12*, 3263–3271. [[CrossRef](#)] [[PubMed](#)]
25. Langecker, M.; Arnaut, V.; Martin, T.G.; List, J.; Renner, S.; Mayer, M.; Dietz, H.; Simmel, F.C. Synthetic lipid membrane channels formed by designed DNA nanostructures. *Science* **2012**, *338*, 932–936. [[CrossRef](#)]
26. Gopfrich, K.; Li, C.Y.; Ricci, M.; Bhamidimarri, S.P.; Yoo, J.; Gyenes, B.; Ohmann, A.; Winterhalter, M.; Aksimentiev, A.; Keyser, U.F. Large-Conductance Transmembrane Porin Made from DNA Origami. *ACS Nano* **2016**, *10*, 8207–8214. [[CrossRef](#)]
27. Diederichs, T.; Pugh, G.; Dorey, A.; Xing, Y.; Burns, J.R.; Nguyen, Q.H.; Tornow, M.; Tampe, R.; Howorka, S. Synthetic protein-conductive membrane nanopores built with DNA. *Nat. Commun.* **2019**, *10*, 5018. [[CrossRef](#)]
28. Thomsen, R.P.; Malle, M.G.; Okholm, A.H.; Krishnan, S.; Bohr, S.S.; Sorensen, R.S.; Ries, O.; Vogel, S.; Simmel, F.C.; Hatzakis, N.S.; et al. A large size-selective DNA nanopore with sensing applications. *Nat. Commun.* **2019**, *10*, 5655. [[CrossRef](#)]
29. Fragasso, A.; De Franceschi, N.; Stommer, P.; van der Sluis, E.O.; Dietz, H.; Dekker, C. Reconstitution of Ultrawide DNA Origami Pores in Liposomes for Transmembrane Transport of Macromolecules. *ACS Nano* **2021**, *15*, 12768–12779. [[CrossRef](#)]
30. Xing, Y.; Dorey, A.; Jayasinghe, L.; Howorka, S. Highly shape- and size-tunable membrane nanopores made with DNA. *Nat. Nanotechnol.* **2022**, *17*, 708–713. [[CrossRef](#)] [[PubMed](#)]
31. Burns, J.R.; Stulz, E.; Howorka, S. Self-assembled DNA nanopores that span lipid bilayers. *Nano Lett.* **2013**, *13*, 2351–2356. [[CrossRef](#)]
32. Burns, J.R.; Gopfrich, K.; Wood, J.W.; Thacker, V.V.; Stulz, E.; Keyser, U.F.; Howorka, S. Lipid-bilayer-spanning DNA nanopores with a bifunctional porphyrin anchor. *Angew. Chem. Int. Ed. Engl.* **2013**, *52*, 12069–12072. [[CrossRef](#)]
33. Debnath, M.; Chakraborty, S.; Kumar, Y.P.; Chaudhuri, R.; Jana, B.; Dash, J. Ionophore constructed from non-covalent assembly of a G-quadruplex and liponucleoside transports  $K^+$ -ion across biological membranes. *Nat. Commun.* **2020**, *11*, 469. [[CrossRef](#)]
34. Krishnan, S.; Ziegler, D.; Dietz, H.; Simmel, F.C. Molecular transport through large-diameter DNA nanopores. *Nat. Commun.* **2016**, *7*, 12787. [[CrossRef](#)]
35. Li, C.; Chen, H.; Zhou, L.; Shi, H.; He, X.; Yang, X.; Wang, K.; Liu, J. Single-stranded DNA designed lipophilic G-quadruplexes as transmembrane channels for switchable potassium transport. *Chem. Commun.* **2019**, *55*, 12004–12007. [[CrossRef](#)]
36. Aldaye, F.A.; Lo, P.K.; Karam, P.; McLaughlin, C.K.; Cosa, G.; Sleiman, H.F. Modular construction of DNA nanotubes of tunable geometry and single- or double-stranded character. *Nat. Nanotechnol.* **2009**, *4*, 349–352. [[CrossRef](#)]
37. Lo, P.K.; Karam, P.; Aldaye, F.A.; McLaughlin, C.K.; Hamblin, G.D.; Cosa, G.; Sleiman, H.F. Loading and selective release of cargo in DNA nanotubes with longitudinal variation. *Nat. Chem.* **2010**, *2*, 319–328. [[CrossRef](#)]
38. Hamblin, G.D.; Carneiro, K.M.M.; Fakhoury, J.F.; Bujold, K.E.; Sleiman, H.F. Rolling Circle Amplification-Templated DNA Nanotubes Show Increased Stability and Cell Penetration Ability. *J. Am. Chem. Soc.* **2012**, *134*, 2888–2891. [[CrossRef](#)]
39. Hariri, A.A.; Hamblin, G.D.; Gidi, Y.; Sleiman, H.F.; Cosa, G. Stepwise growth of surface-grafted DNA nanotubes visualized at the single-molecule level. *Nat. Chem.* **2015**, *7*, 295–300. [[CrossRef](#)]
40. Rahbani, J.F.; Vengut-Climent, E.; Chidchob, P.; Gidi, Y.; Trinh, T.; Cosa, G.; Sleiman, H.F. DNA Nanotubes with Hydrophobic Environments: Toward New Platforms for Guest Encapsulation and Cellular Delivery. *Adv. Health Mater.* **2018**, *7*, 1701049. [[CrossRef](#)]
41. Saliba, D.; Luo, X.; Rizzuto, F.J.; Sleiman, H.F. Programming rigidity into size-defined wireframe DNA nanotubes. *Nanoscale* **2023**, *15*, 5403–5413. [[CrossRef](#)]
42. Yang, Q.; Guo, Z.; Liu, H.; Peng, R.; Xu, L.; Bi, C.; He, Y.; Liu, Q.; Tan, W. A Cascade Signaling Network between Artificial Cells Switching Activity of Synthetic Transmembrane Channels. *J. Am. Chem. Soc.* **2020**, *143*, 232–240. [[CrossRef](#)]
43. Yoo, J.; Aksimentiev, A. Molecular Dynamics of Membrane-Spanning DNA Channels: Conductance Mechanism, Electro-Osmotic Transport, and Mechanical Gating. *J. Phys. Chem. Lett.* **2015**, *6*, 4680–4687. [[CrossRef](#)]
44. Maingi, V.; Lelimosin, M.; Howorka, S.; Sansom, M.S.P. Gating-like Motions and Wall Porosity in a DNA Nanopore Scaffold Revealed by Molecular Simulations. *ACS Nano* **2015**, *9*, 11209–11217. [[CrossRef](#)] [[PubMed](#)]
45. Maingi, V.; Burns, J.R.; Uusitalo, J.J.; Howorka, S.; Marrink, S.J.; Sansom, M.S. Stability and dynamics of membrane-spanning DNA nanopores. *Nat. Commun.* **2017**, *8*, 14784. [[CrossRef](#)] [[PubMed](#)]
46. Birkholz, O.; Burns, J.R.; Richter, C.P.; Psathaki, O.E.; Howorka, S.; Piehler, J. Multi-functional DNA nanostructures that puncture and remodel lipid membranes into hybrid materials. *Nat. Commun.* **2018**, *9*, 1521. [[CrossRef](#)] [[PubMed](#)]
47. Luo, L.; Manda, S.; Park, Y.; Demir, B.; Sanchez, J.; Anantram, M.P.; Oren, E.E.; Gopinath, A.; Rolandi, M. DNA nanopores as artificial membrane channels for bioprotonics. *Nat. Commun.* **2023**, *14*, 5364. [[CrossRef](#)] [[PubMed](#)]

48. Diederichs, T.; Ahmad, K.; Burns, J.R.; Nguyen, Q.H.; Siwy, Z.S.; Tornow, M.; Coveney, P.V.; Tampe, R.; Howorka, S. Principles of Small-Molecule Transport through Synthetic Nanopores. *ACS Nano* **2021**, *15*, 16194–16206. [[CrossRef](#)]
49. Gopfrich, K.; Zettl, T.; Meijering, A.E.; Hernandez-Ainsa, S.; Kocabay, S.; Liedl, T.; Keyser, U.F. DNA-Tile Structures Induce Ionic Currents through Lipid Membranes. *Nano Lett.* **2015**, *15*, 3134–3138. [[CrossRef](#)]
50. Mathieu, F.; Liao, S.; Kopatsch, J.; Wang, T.; Mao, C.; Seeman, N.C. Six-Helix Bundles Designed from DNA. *Nano Lett.* **2005**, *5*, 661–665. [[CrossRef](#)]
51. Endo, M.; Seeman, N.C.; Majima, T. DNA Tube Structures Controlled by a Four-Way-Branched DNA Connector. *Angew. Chem. Int. Ed. Engl.* **2005**, *44*, 6074–6077. [[CrossRef](#)]
52. Mohammed, A.M.; Šulc, P.; Zenk, J.; Schulman, R. Self-assembling DNA nanotubes to connect molecular landmarks. *Nat. Nanotechnol.* **2016**, *12*, 312–316. [[CrossRef](#)] [[PubMed](#)]
53. Green, L.N.; Subramanian, H.K.K.; Mardanlou, V.; Kim, J.; Hariadi, R.F.; Franco, E. Autonomous dynamic control of DNA nanostructure self-assembly. *Nat. Chem.* **2019**, *11*, 510–520. [[CrossRef](#)] [[PubMed](#)]
54. Agarwal, S.; Franco, E. Enzyme-Driven Assembly and Disassembly of Hybrid DNA-RNA Nanotubes. *J. Am. Chem. Soc.* **2019**, *141*, 7831–7841. [[CrossRef](#)] [[PubMed](#)]
55. Jia, S.; Phua, S.C.; Nihongaki, Y.; Li, Y.; Pacella, M.; Li, Y.; Mohammed, A.M.; Sun, S.; Inoue, T.; Schulman, R. Growth and site-specific organization of micron-scale biomolecular devices on living mammalian cells. *Nat. Commun.* **2021**, *12*, 5729. [[CrossRef](#)]
56. Dhanasekar, N.N.; Li, Y.; Schulman, R. The ion permeability of DNA nanotube channels. *BioRxiv* **2022**, 1–33. [[CrossRef](#)]
57. Li, Y.; Maffeo, C.; Schulman, R. Leakless end-to-end transport of small molecules through micron-length DNA nanochannels. *Sci. Adv.* **2022**, *8*, eabq4834. [[CrossRef](#)]
58. Rothmund, P.W. Folding DNA to create nanoscale shapes and patterns. *Nature* **2006**, *440*, 297–302. [[CrossRef](#)]
59. Forman, S.L.; Fettingner, J.C.; Pieraccini, S.; Gottarelli, G.; Davis, J.T. Toward Artificial Ion Channels: A Lipophilic G-Quadruplex. *J. Am. Chem. Soc.* **2000**, *122*, 4060–4067. [[CrossRef](#)]
60. Lee, M.P.H.; Parkinson, G.N.; Hazel, P.; Neidle, S. Observation of the Coexistence of Sodium and Calcium Ions in a DNA G-Quadruplex Ion Channel. *J. Am. Chem. Soc.* **2007**, *129*, 10106–10107. [[CrossRef](#)]
61. Akhshi, P.; Mosey, N.J.; Wu, G. Free-Energy Landscapes of Ion Movement through a G-Quadruplex DNA Channel. *Angew. Chem.* **2012**, *124*, 2904–2908. [[CrossRef](#)]
62. Akhshi, P.; Wu, G. Umbrella sampling molecular dynamics simulations reveal concerted ion movement through G-quadruplex DNA channels. *Phys. Chem. Chem. Phys.* **2017**, *19*, 11017–11025. [[CrossRef](#)] [[PubMed](#)]
63. Balasubramanian, S.; Senapati, S. Dynamics and Barrier of Movements of Sodium and Potassium Ions Across the Oxytricha nova G-Quadruplex Core. *J. Phys. Chem. B* **2020**, *124*, 11055–11066. [[CrossRef](#)]
64. Göpfrich, K.; Li, C.-Y.; Mames, I.; Bhamidimarri, S.P.; Ricci, M.; Yoo, J.; Mames, A.; Ohmann, A.; Winterhalter, M.; Stulz, E.; et al. Ion Channels Made from a Single Membrane-Spanning DNA Duplex. *Nano Lett.* **2016**, *16*, 4665–4669. [[CrossRef](#)]
65. Morzy, D.; Joshi, H.; Sandler, S.E.; Aksimentiev, A.; Keyser, U.F. Membrane Activity of a DNA-Based Ion Channel Depends on the Stability of Its Double-Stranded Structure. *Nano Lett.* **2021**, *21*, 9789–9796. [[CrossRef](#)] [[PubMed](#)]
66. Burns, J.R.; Seifert, A.; Fertig, N.; Howorka, S. A biomimetic DNA-based channel for the ligand-controlled transport of charged molecular cargo across a biological membrane. *Nat. Nanotechnol.* **2016**, *11*, 152–156. [[CrossRef](#)]
67. Dey, S.; Dorey, A.; Abraham, L.; Xing, Y.; Zhang, I.; Zhang, F.; Howorka, S.; Yan, H. A reversibly gated protein-transporting membrane channel made of DNA. *Nat. Commun.* **2022**, *13*, 2271. [[CrossRef](#)]
68. Seifert, A.; Gopfrich, K.; Keyser, U.F.; Howorka, S. Bilayer-Spanning DNA Nanopores with Voltage-Switching between Open and Closed State. *ACS Nano* **2015**, *9*, 1117–1126. [[CrossRef](#)]
69. Iwabuchi, S.; Kawamata, I.; Murata, S.; Nomura, S.M. A large, square-shaped, DNA origami nanopore with sealing function on a giant vesicle membrane. *Chem. Commun.* **2021**, *57*, 2990–2993. [[CrossRef](#)]
70. Lanphere, C.; Ciccone, J.; Dorey, A.; Hagleitner-Ertugrul, N.; Knyazev, D.; Haider, S.; Howorka, S. Triggered Assembly of a DNA-Based Membrane Channel. *J. Am. Chem. Soc.* **2022**, *144*, 4333–4344. [[CrossRef](#)]
71. Yang, L.; Cullin, C.; Elezgaray, J. Detection of Short DNA Sequences with DNA Nanopores. *Chemphyschem* **2022**, *23*, e202200021. [[CrossRef](#)] [[PubMed](#)]
72. Mendoza, O.; Calmet, P.; Alves, I.; Lecomte, S.; Raoux, M.; Cullin, C.; Elezgaray, J. A tensegrity driven DNA nanopore. *Nanoscale* **2017**, *9*, 9762–9769. [[CrossRef](#)] [[PubMed](#)]
73. Arnott, P.M.; Howorka, S. A Temperature-Gated Nanovalve Self-Assembled from DNA to Control Molecular Transport across Membranes. *ACS Nano* **2019**, *13*, 3334–3340. [[CrossRef](#)] [[PubMed](#)]
74. Li, P.; Xie, G.; Kong, X.Y.; Zhang, Z.; Xiao, K.; Wen, L.; Jiang, L. Light-Controlled Ion Transport through Biomimetic DNA-Based Channels. *Angew. Chem. Int. Ed. Engl.* **2016**, *55*, 15637–15641. [[CrossRef](#)]
75. Offenbartl-Stiegert, D.; Rottensteiner, A.; Dorey, A.; Howorka, S. A Light-Triggered Synthetic Nanopore for Controlling Molecular Transport Across Biological Membranes. *Angew. Chem. Int. Ed. Engl.* **2022**, *61*, e202210886. [[CrossRef](#)]
76. Li, C.; Chen, H.; Yang, X.; Wang, K.; Liu, J. An ion transport switch based on light-responsive conformation-dependent G-quadruplex transmembrane channels. *Chem. Commun.* **2021**, *57*, 8214–8217. [[CrossRef](#)]
77. Li, C.; Chen, H.; Chen, Q.; Shi, H.; Yang, X.; Wang, K.; Liu, J. Lipophilic G-Quadruplex Isomers as Biomimetic Ion Channels for Conformation-Dependent Selective Transmembrane Transport. *Anal. Chem.* **2020**, *92*, 10169–10176. [[CrossRef](#)] [[PubMed](#)]

78. Lin, C.; Wu, G.; Wang, K.; Onel, B.; Sakai, S.; Shao, Y.; Yang, D. Molecular Recognition of the Hybrid-2 Human Telomeric G-Quadruplex by Epiberberine: Insights into Conversion of Telomeric G-Quadruplex Structures. *Angew. Chem. Int. Ed. Engl.* **2018**, *57*, 10888–10893. [[CrossRef](#)]
79. Lu, H.; Li, S.; Chen, J.; Xia, J.; Zhang, J.; Huang, Y.; Liu, X.; Wu, H.; Zhao, Y.; Chaia, Z.; et al. Metal ions modulate the conformation and stability of a G-quadruplex with or without a small-molecule ligand. *Metallomics* **2015**, *7*, 1508–1514. [[CrossRef](#)]
80. Messenger, L.; Burns, J.R.; Kim, J.; Cecchin, D.; Hindley, J.; Pyne, A.L.; Gaitzsch, J.; Battaglia, G.; Howorka, S. Biomimetic Hybrid Nanocontainers with Selective Permeability. *Angew. Chem. Int. Ed. Engl.* **2016**, *55*, 11106–11109. [[CrossRef](#)]
81. Burns, J.R.; Al-Juffali, N.; Janes, S.M.; Howorka, S. Membrane-spanning DNA nanopores with cytotoxic effect. *Angew. Chem. Int. Ed. Engl.* **2014**, *53*, 12466–12470. [[CrossRef](#)] [[PubMed](#)]
82. Lv, C.; Gu, X.; Li, H.; Zhao, Y.; Yang, D.; Yu, W.; Han, D.; Li, J.; Tan, W. Molecular Transport through a Biomimetic DNA Channel on Live Cell Membranes. *ACS Nano* **2020**, *14*, 14616–14626. [[CrossRef](#)] [[PubMed](#)]
83. Chen, L.; Liang, S.; Chen, Y.; Wu, M.; Zhang, Y. Destructing the Plasma Membrane with Activatable Vesicular DNA Nanopores. *ACS Appl. Mater. Interfaces* **2020**, *12*, 96–105. [[CrossRef](#)] [[PubMed](#)]
84. Lanphere, C.; Arnott, P.M.; Jones, S.F.; Korlova, K.; Howorka, S. A Biomimetic DNA-Based Membrane Gate for Protein-Controlled Transport of Cytotoxic Drugs. *Angew. Chem. Int. Ed. Engl.* **2021**, *60*, 1903–1908. [[CrossRef](#)] [[PubMed](#)]
85. Chen, Q.; Jian, M.; Chen, H.; Zhou, B.; Shi, H.; Yang, X.; Wang, K.; Liu, J. Design of Lipophilic Split Aptamers as Artificial Carriers for Transmembrane Transport of Adenosine Triphosphate. *CCS Chem.* **2021**, *3*, 144–153. [[CrossRef](#)]
86. Veetil, A.T.; Chakraborty, K.; Xiao, K.; Minter, M.R.; Sisodia, S.S.; Krishnan, Y. Cell-targetable DNA nanocapsules for spatiotemporal release of caged bioactive small molecules. *Nat. Nanotechnol.* **2017**, *12*, 1183–1189. [[CrossRef](#)] [[PubMed](#)]
87. Xie, G.; Li, P.; Zhao, Z.; Kong, X.Y.; Zhang, Z.; Xiao, K.; Wang, H.; Wen, L.; Jiang, L. Bacteriorhodopsin-Inspired Light-Driven Artificial Molecule Motors for Transmembrane Mass Transportation. *Angew. Chem. Int. Ed. Engl.* **2018**, *57*, 16708–16712. [[CrossRef](#)]
88. List, J.; Weber, M.; Simmel, F.C. Hydrophobic actuation of a DNA origami bilayer structure. *Angew. Chem. Int. Ed. Engl.* **2014**, *53*, 4236–4239. [[CrossRef](#)]
89. Bennett, I.M.; Farfano, H.M.V.; Bogani, F.; Primak, A.; Liddell, P.A.; Otero, L.; Sereno, L.; Silber, J.J.; Moore, A.L.; Moore, T.A.; et al. Active transport of Ca<sup>2+</sup> by an artificial photosynthetic membrane. *Nature* **2002**, *420*, 398–401. [[CrossRef](#)]
90. Cui, C.; Chakraborty, K.; Tang, X.A.; Schoenfelt, K.Q.; Hoffman, A.; Blank, A.; McBeth, B.; Pulliam, N.; Reardon, C.A.; Kulkarni, S.A.; et al. A lysosome-targeted DNA nanodevice selectively targets macrophages to attenuate tumours. *Nat. Nanotechnol.* **2021**, *16*, 1394–1402. [[CrossRef](#)]
91. Maffeo, C.; Quednau, L.; Wilson, J.; Aksimentiev, A. DNA double helix, a tiny electromotor. *Nat. Nanotechnol.* **2022**, *18*, 238–242. [[CrossRef](#)] [[PubMed](#)]
92. Wang, L.; Guo, P.; Jin, D.; Peng, Y.; Sun, X.; Chen, Y.; Liu, X.; Chen, W.; Wang, W.; Yan, X.; et al. Enzyme-Powered Tubular Microrobotic Jets as Bioinspired Micropumps for Active Transmembrane Drug Transport. *ACS Nano* **2023**, *17*, 5095–5107. [[CrossRef](#)] [[PubMed](#)]
93. Yang, J.; Yu, G.; Sessler, J.L.; Shin, I.; Gale, P.A.; Huang, F. Artificial transmembrane ion transporters as potential therapeutics. *Chem* **2021**, *7*, 3256–3291. [[CrossRef](#)]
94. Kanner, S.A.; Shuja, Z.; Choudhury, P.; Jain, A.; Colecraft, H.M. Targeted deubiquitination rescues distinct trafficking-deficient ion channelopathies. *Nat. Methods* **2020**, *17*, 1245–1253. [[CrossRef](#)] [[PubMed](#)]
95. Rastergar, A.; Soleimani, M. Hypokalaemia and hyperkalaemia. *Postgrad. Med. J.* **2001**, *77*, 759–764. [[CrossRef](#)]
96. Curran, J.; Mohler, P.J. Alternative paradigms for ion channelopathies: Disorders of ion channel membrane trafficking and posttranslational modification. *Annu. Rev. Physiol.* **2015**, *77*, 505–524. [[CrossRef](#)]

**Disclaimer/Publisher’s Note:** The statements, opinions and data contained in all publications are solely those of the individual author(s) and contributor(s) and not of MDPI and/or the editor(s). MDPI and/or the editor(s) disclaim responsibility for any injury to people or property resulting from any ideas, methods, instructions or products referred to in the content.